MULTI-MESSENGER INSIGHTS INTO ULTRA-HIGH-ENERGY COSMIC RAYS FROM FR0 RADIO GALAXIES:

EMISSION SPECTRUM, COMPOSITION, AND SECONDARY PHOTONS AND NEUTRINOS

Jon Paul Lundquist
jplundquist@gmail.com

University of
Nova Gorica

www.ung.si/en/research/cac/

"Combined Fit of Spectrum and Composition for FR0 Radio Galaxy Emitted Ultra-High-Energy Cosmic Rays with Resulting Secondary Photons and Neutrinos"

arXiv:2407.06961 Accepted for Publication in ApJ

Jon Paul Lundquist[1], Serguei Vorobiov[1], Lukas Merten[2], Anita Reimer[2], Margot Boughelilba[2], Paolo Da Vela[2], Fabrizio Tavecchio[3], Giacomo Bonnoli [3], Chiara Righi[3]

[1]*Center for Astrophysics and Cosmology (CAC), University of Nova Gorica, Nova Gorica, Slovenia*
[2]*Institute for Astro and Particle Physics, University of Innsbruck, Innsbruck, Austria*
[3]*Astronomical Observatory of Brera, Milano, Italy*

University of Nova Gorica

universität innsbruck

INAF ISTITUTO NAZIONALE DI ASTROFISICA

ABSTRACT SUMMARY

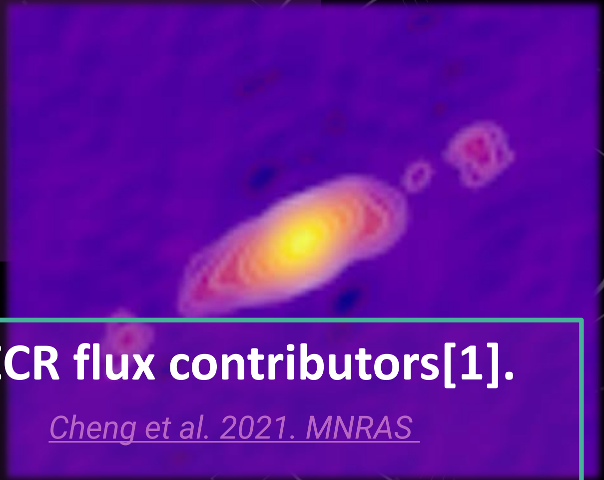

Cheng et al. 2021. MNRAS

- Low luminosity Fanaroff-Riley Type 0 (FR0) radio galaxies can be significant UHECR flux contributors[1].
  - FR0 outnumber more powerful FR radio galaxies by $\sim 5\times$ (z<0.05).
- This comprehensive CRPropa3 simulation study estimates FR0 emitted UHECR mass composition and energy spectra.
  - Integrates FR0 properties[2] and intergalactic magnetic fields (random and structured).
- Fitting spectral indices, rigidity cutoffs, and elemental fractions to Pierre Auger Observatory's spectrum and composition, probes the FR0 source contribution.
- Secondary photon and neutrino fluxes from cosmic photon background interactions are compared with current upper limits and theoretical models.
- This multi-messenger approach provides insights into the role of FR0 within the UHECR landscape.

[1] Merten, L. et al., Scrutinizing FR 0 radio galaxies as ultra-high-energy cosmic ray source candidates, Astropart. Phys. 128 (2021) 102564.
[2] Baldi, R. D. et al., FR0CAT: a FIRST catalog of FR 0 radio galaxies, A&A 609 (2018) A1.

ISOTROPIC FR-0 SIMULATION

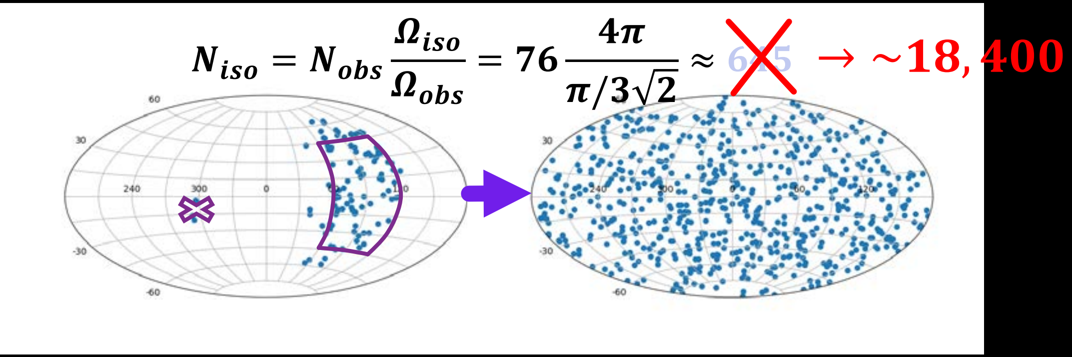

Full-sky isotropic FR0 radio galaxy density estimated from well-sampled FR0CAT[1] catalog section.

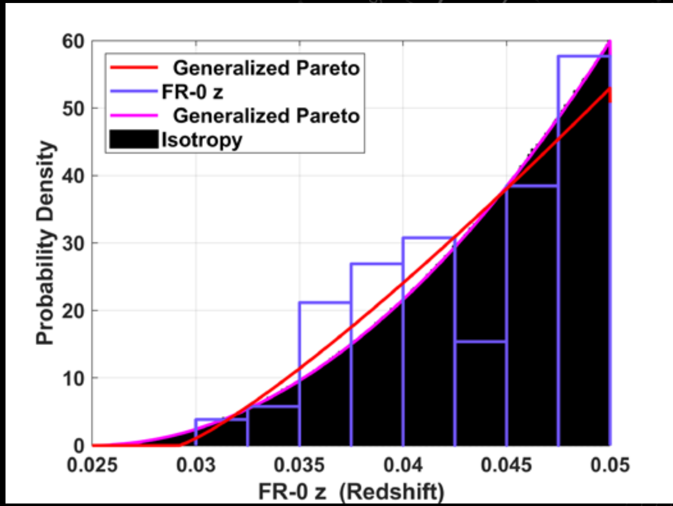

Simulated FR0 redshift distribution from Pareto fit to catalog data[1]. Isotropy p-val = 16%.

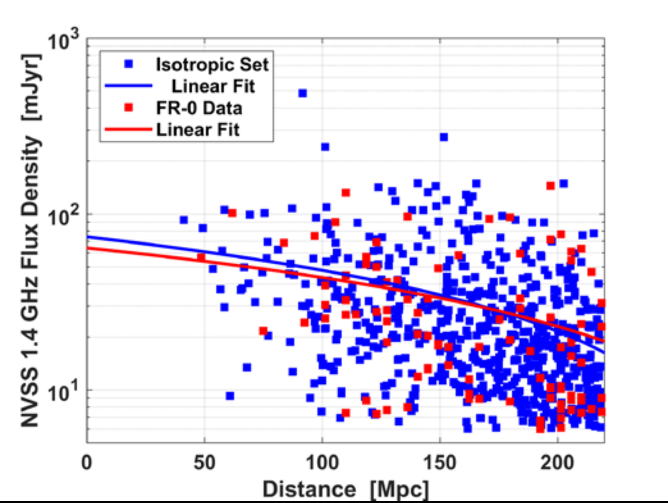

Previous results:
$z \leq 0.05$
Update:
$z \leq 0.2$

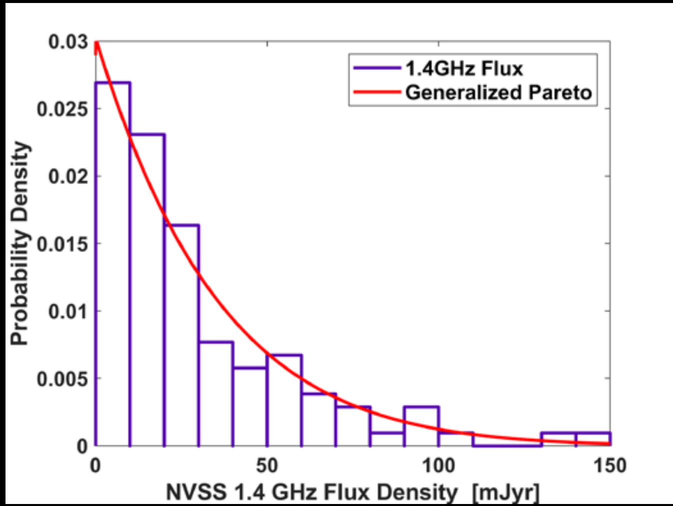

Source evolution modeled by preserving radio output and redshift-distance correlation (Kendall Corr. Coeff: -0.28, p-val: 4.6e-5)[1].

FR0 UHECR flux proportional to radio output. Generated by Pareto fit to NVSS data[1].

CONSTANT FRACTION FIT

MODELS AND COMBINED FIT – CONSTANT FRACTION

- **Three EAS Models**: SIBYLL2.3c, EPOS-LHC and QGSJETII-04
- **Two Structured Fields**:
  - Dolag et al. arXiv:0410419
  - CLUES -- Hackenstein et al. (Astro_1B): arXiv:1710.01353
- **Two 1 nG Random Fields**:
  - A: $\langle l_{\text{corr}} \rangle = 234$ kpc, B: $\langle l_{\text{corr}} \rangle = 647$ kpc
- **And No Magnetic Field**

Tables in appendix

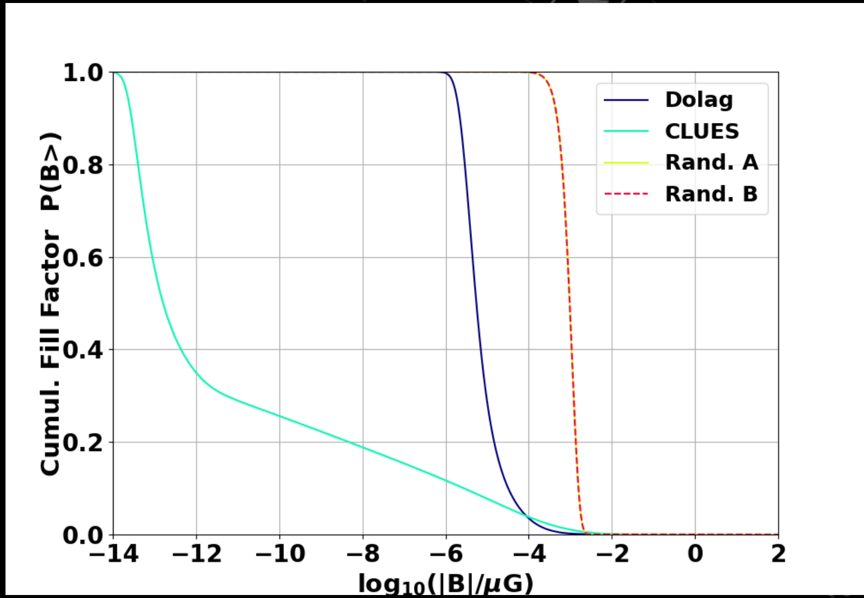

Minimize

$$\sum \chi^2_{tot}/dof = \sum \chi^2_E/dof_E + \sum \chi^2_C/dof_C$$

- **8 Parameters**
  - Power Law: γ
  - Spectrum Normalization: n
  - Rigidity-Dependent Exponential Cutoff: ZR_{cut}
  - **5 nuclei fit:** H, He, N, Si, Fe
    - $\sum f_a = 100\% \rightarrow$ **4 parameters**
  - Maximum Trajectory D

- CRPropa3 Sim. Power Law $\gamma = 1$
- Reweight Simulated Events

$$\frac{\mathrm{d}N_A}{\mathrm{d}E} = J_A(E) = f_A J_0 \left(\frac{E}{10^{18}\ \mathrm{eV}}\right)^{-\gamma} \times f_{\text{cut}}(E, Z_A R_{\text{cut}})$$

$$f_{\text{cut}}(E, Z_A R_{\text{cut}}) = \begin{cases} 1 & (E < Z_A R_{\text{cut}}) \\ \exp\left(1 - \frac{E}{Z_A R_{\text{cut}}}\right) & (E > Z_A R_{\text{cut}}) \end{cases}$$

- Constant Nuclei Fractions: f_A
- Rigidity Dependent Cutoff: ZR_{cut}

Auger JCAP (2017) arXiv:1612.07155

ENERGY SPECTRUM AND ⟨lnA⟩ FITS

***Data from*:**
Deligny, O. et al., *PoS* ICRC2019 (2020) 234
Yushkov, A. et al., *PoS* ICRC2019 (2020) 482

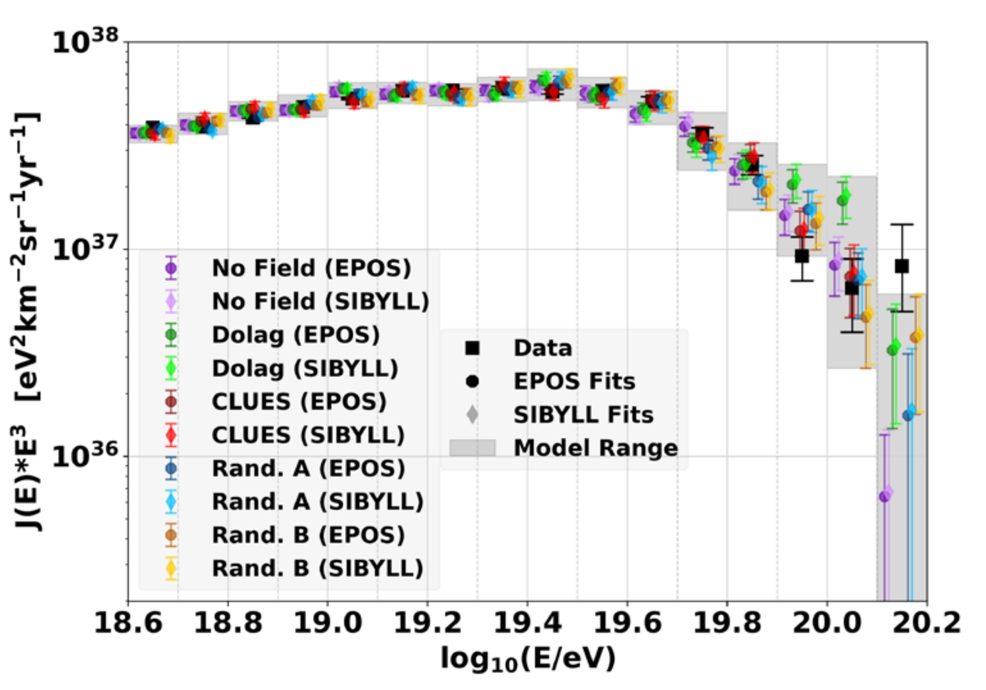

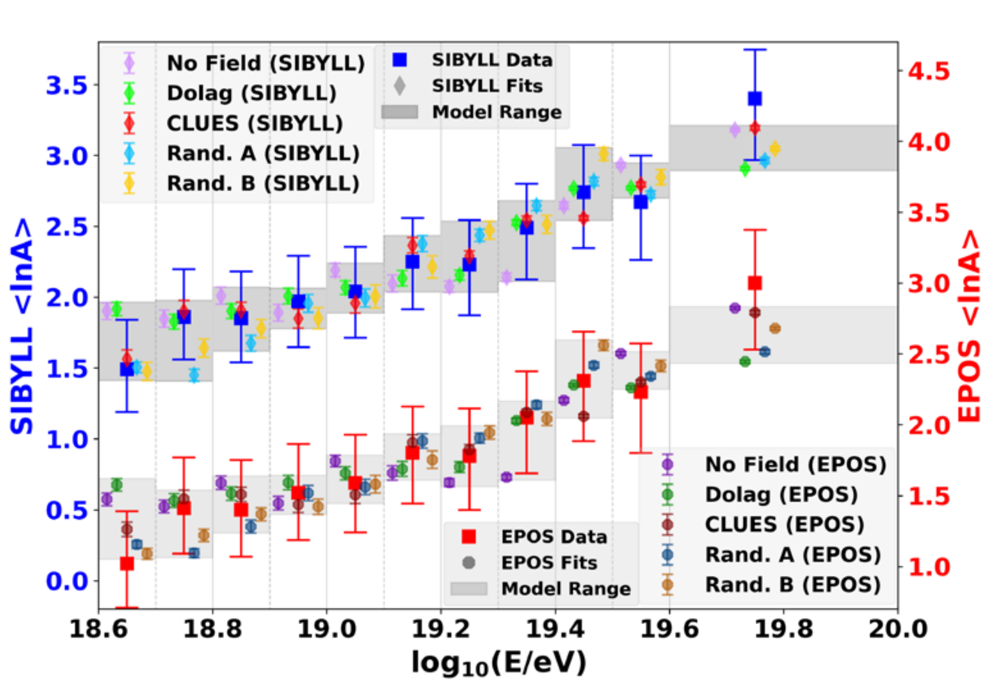

- Energy spectra for 10 models.
- Highest energies are not well fit.
  - FR0 not expected as a significant contributor.
  - Contribution from other sources? SGBs? (Abdul Halim et al. 2024)

- ⟨lnA⟩ for 10 models.
- Largest residuals: First and last energy bin.

FIT PARAMETER RESULTS VS MAGNETIC FIELD

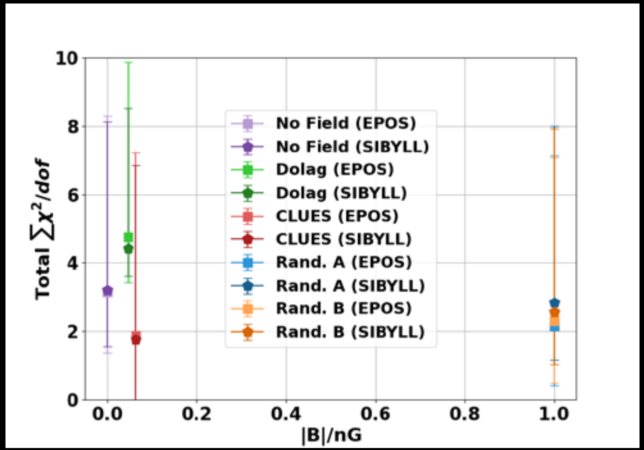

Goodness-of-fit

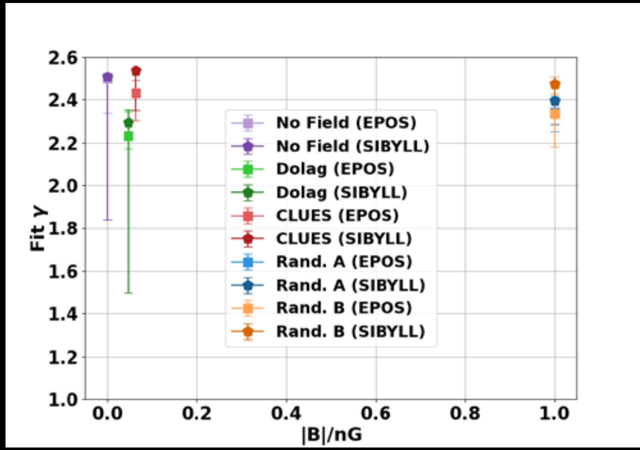

Power law Spectral Index γ

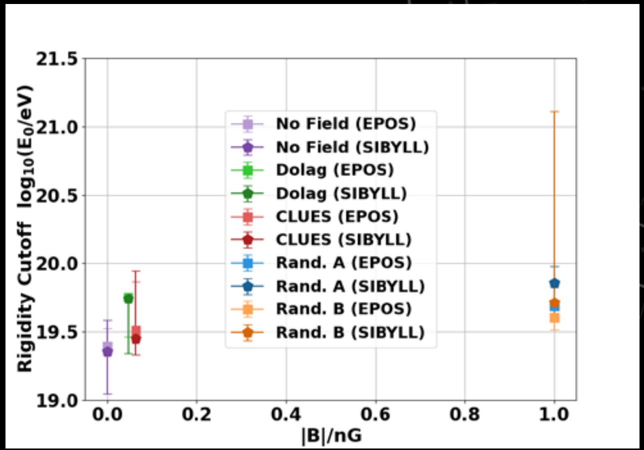

Rigidity cutoff R_{cut}

Error bars: 1 Gaussian σ C.I. around best fit for bootstrapped sims & Gaussian sampled data.

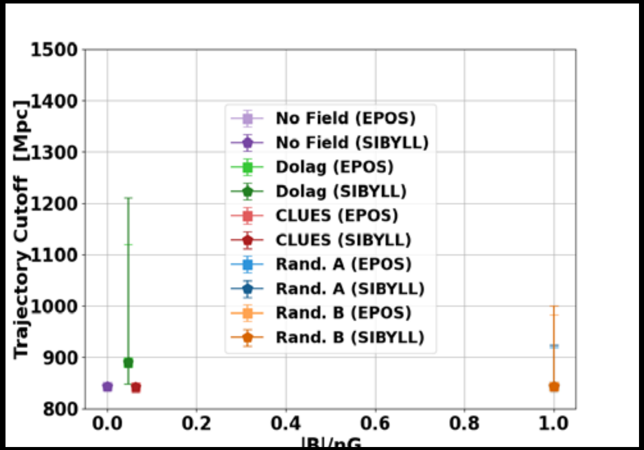

Trajectory cutoff D_{cut}

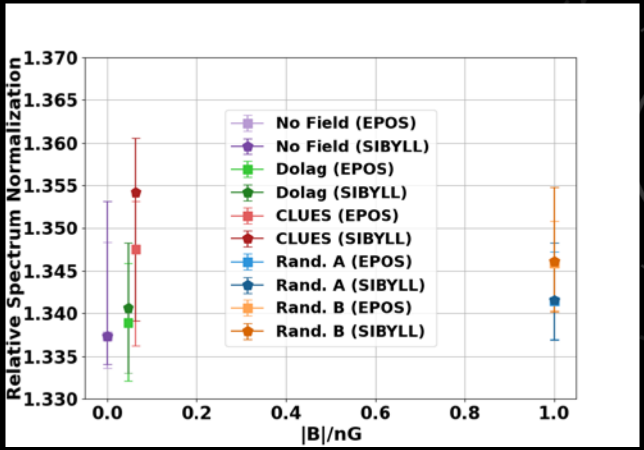

Spectrum Normalization

EMITTED NUCLEI FRACTIONS

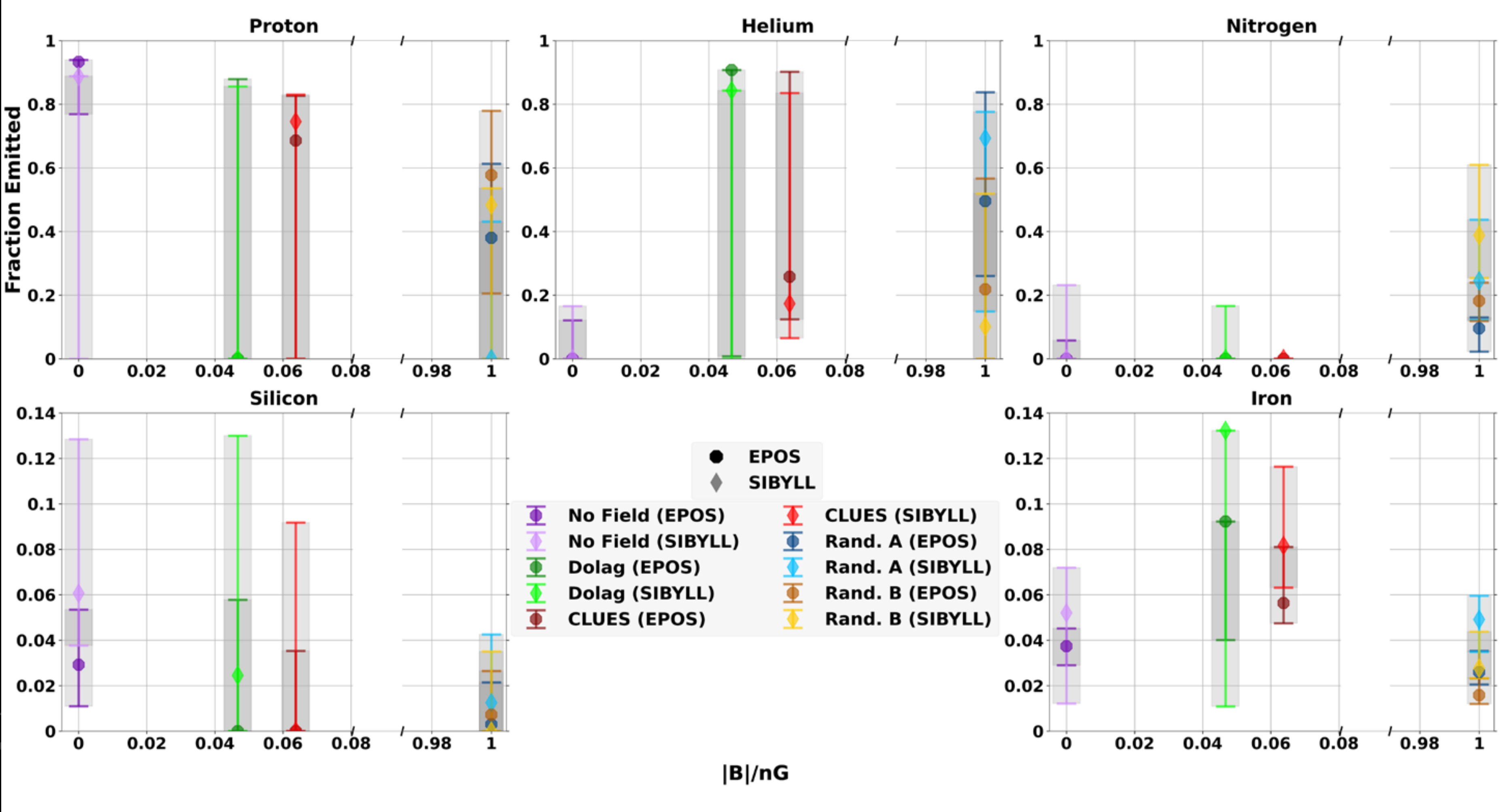

Combined Light Nuclei

Field	Model	$f_H(\%) + f_{He}(\%)$
No Field	SIBYLL	$88.7^{+0.2}_{-24.0}$
	EPOS	$93.4^{+0.7}_{-7.2}$
	QGS4	$97.6^{+0.3}_{-1.1}$
Dolag	SIBYLL	$84.3^{+5.2}_{-11.9}$
	EPOS	$90.8^{+3.7}_{-3.8}$
	QGS4	$97.1^{+0.4}_{-1.0}$
CLUES	SIBYLL	$91.8^{+0.3}_{-11.4}$
	EPOS	$94.4^{+0.4}_{-4.4}$
	QGS4	$97.4^{+0.4}_{-0.5}$
Rand.A	SIBYLL	$69.3^{+11.1}_{-19.2}$
	EPOS	$87.6^{+5.6}_{-4.2}$
	QGS4	$98.9^{+0.0}_{-3.5}$
Rand.B	SIBYLL	$58.4^{+10.5}_{-23.6}$
	EPOS	$79.5^{+5.8}_{-6.5}$
	QGS4	$95.8^{+1.7}_{-4.5}$

***Emitted* Nuclei Fraction Versus Magnetic Field**

PHOTONS – (CLUES–SIBYLL CONFIGURATION)

CLUES–SIBYLL

Red/green areas are no magnetic field and GZK only.

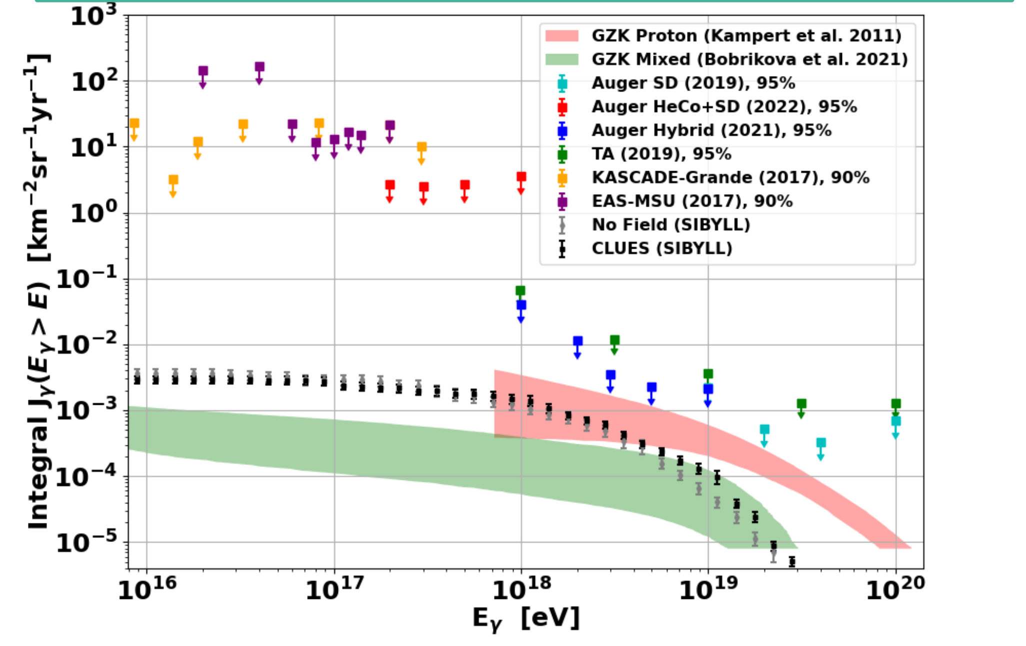

"A Search for Photons with Energies Above 2×10^17 eV Using Hybrid Data from the Low-Energy Extensions of the Pierre Auger Observatory"
P. Abreu et al 2022 ApJ 933 125
arXiv:2205.14864

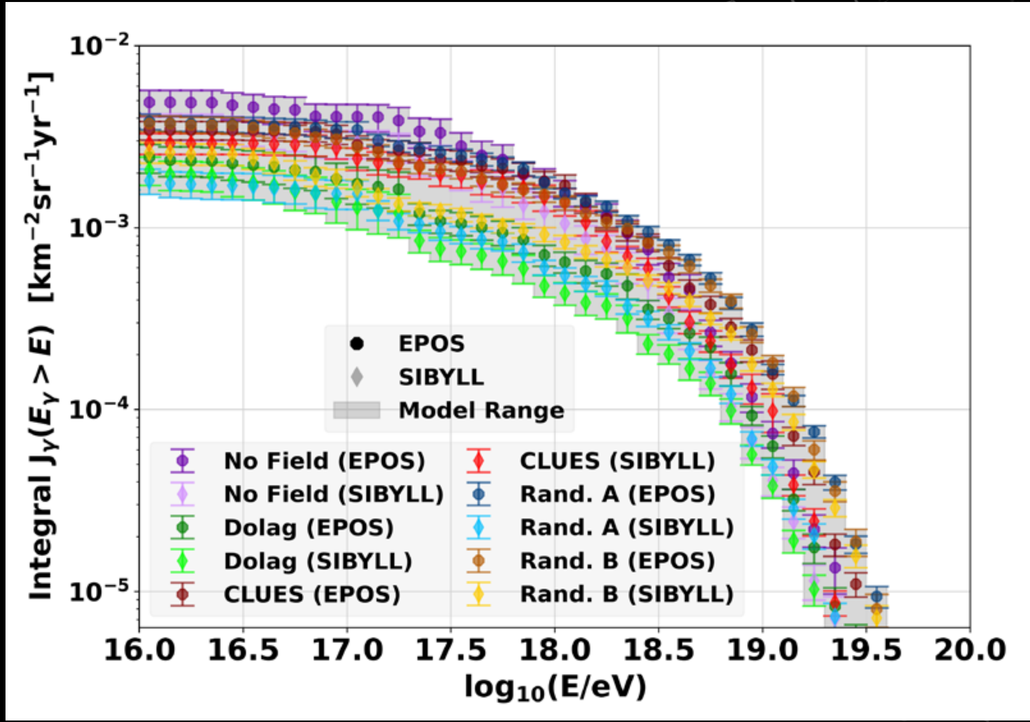

Integral photon flux for 10 models

NEUTRINOS – (CLUES-SIBYLL CONFIGURATION)

CLUES–SIBYLL

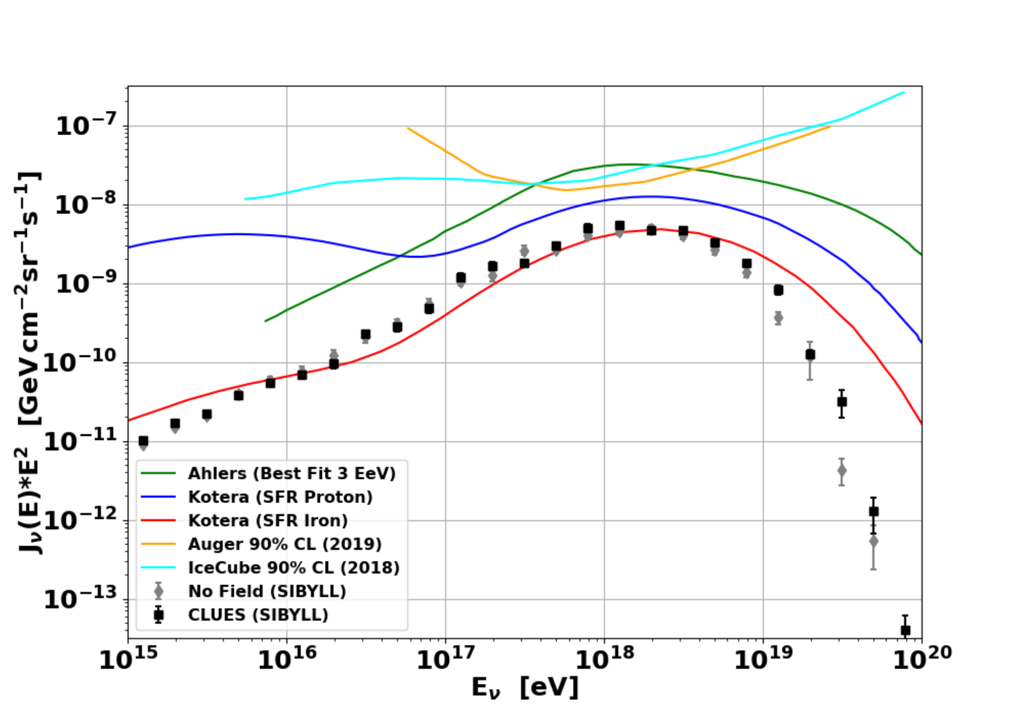

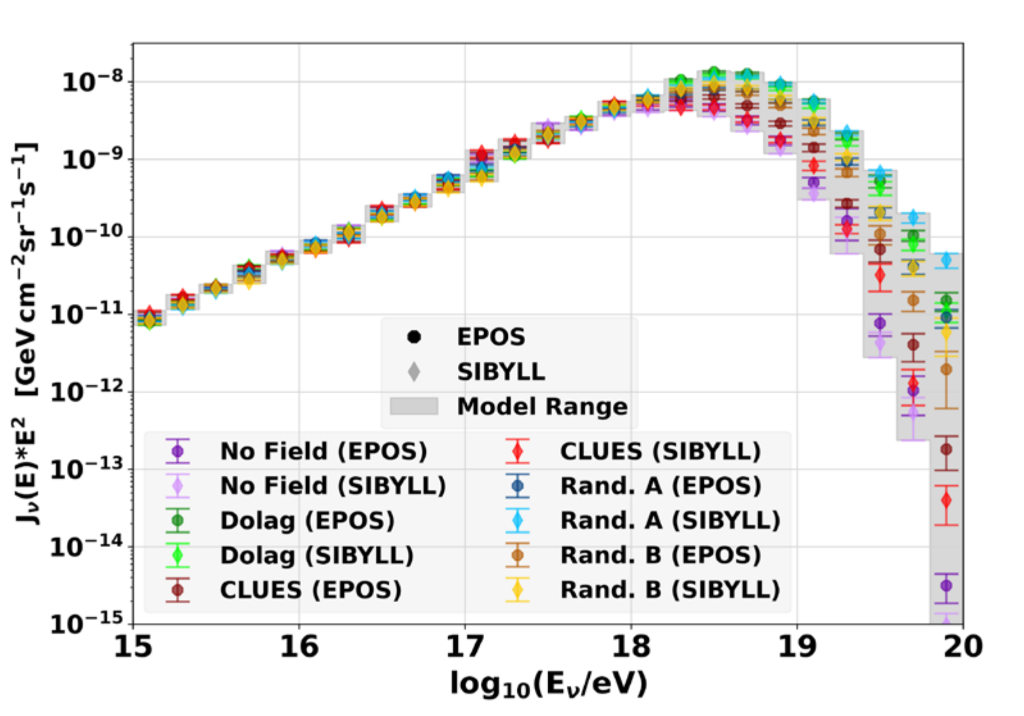

Kotera et al: JCAP (2010) arXiv:1009.1382
Ahlers et al: Astropart.Phys.(2010) arXiv:1005.2620v2
IceCube: Phys.Rev.D(2018) arXiv:1807.01820v2
Auger: JCAP10 (2019) arXiv:1906.07422v2

Neutrino flux for 10 models

CONSTANT FRACTION CONCLUSIONS

Best Fit: CLUES Structured Field with SIBYLL EAS model.

- Next best: CLUES structured field with EPOS EAS model.
- Generally EPOS is the best fit – third: Rand.A-EPOS, fourth: Rand.B-EPOS

***General* trends with increasing magnetic field strength:**

- Small increase: γ
- Small decrease: R_{cut}
- Increases: Helium and Nitrogen emission.
- Decreases: Proton, Silicon, and Iron emission.
- Small decrease: Proton+Helium emission.

Very good fits for CLUES and 1 nG fields with EPOS -- still may require another source type at highest energies.

Photon spectra: higher flux than expected for mixed composition from GZK only.

- Flux increases with magnetic fields at highest energies.
- Below experimental limits.

***Neutrino spectra: lower flux than expected* from Kotera model for mixed composition.**

- Flux generally increases with magnetic fields at highest energies.
- Below experimental limits

EVOLVING FRACTION FIT

COMBINED FIT – *EVOLVING FRACTIONS*

- **Two EAS Models: SIBYLL2.3c, EPOS-LHC**
- **Two Structured Fields:**
  - **Dolag et al.** arXiv:0410419
  - **CLUES -- Hackenstein et al. (Astro_1B):** arXiv:1710.01353
- **Two 1 nG Random Fields:**
  - **A:** $\langle l_{corr} \rangle = 234$ kpc, **B:** $\langle l_{corr} \rangle = 647$ kpc
- **And No Magnetic Field**

Minimize: $\sum \chi^2_{tot}/dof = \sum \chi^2_E/dof_E + \sum \chi^2_C/dof_C$

$$= \sum \chi^2_E/16 + \sum \chi^2_C/11$$

16 energy and 11 composition bins

- **48 Parameters**
  - **Power Law:** γ
  - **Spectrum Normalization:** n
  - **Rigidity-Dependent Exponential Cutoff:** ZR_{cut}
  - **5 nuclei fit: H, He, N, Si, Fe**
    - $\sum f_a(E) = 100\% \rightarrow$ **44 parameters**
  - **Maximum Trajectory** D

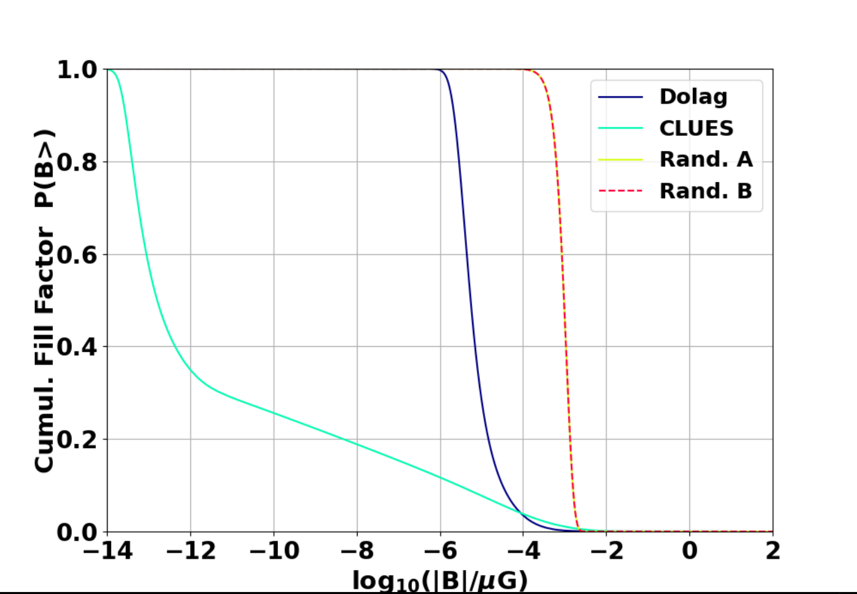

- **CRPropa3 Sim. Power Law** $\gamma = 1$
- **Reweight Simulated Events**

$$\frac{dN_A}{dE} = J_A(E) = f_A J_0 \left(\frac{E}{10^{18}\ \mathrm{eV}}\right)^{-\gamma} \times f_{\mathrm{cut}}(E, Z_A R_{\mathrm{cut}})$$

$$f_{\mathrm{cut}}(E, Z_A R_{\mathrm{cut}}) = \begin{cases} 1 & (E < Z_A R_{\mathrm{cut}}) \\ \exp\left(1 - \frac{E}{Z_A R_{\mathrm{cut}}}\right) & (E > Z_A R_{\mathrm{cut}}) \end{cases}$$

- **Nuclei Fractions:** $f_A(E_{obs})$
- **Rigidity-Dependent Cutoff:** ZR_{cut}

ENERGY SPECTRUM AND ⟨lnA⟩ FITS

Data from:
Deligny, O. et al., *PoS* ICRC2019 (2020) 234
Yushkov, A. et al., *PoS* ICRC2019 (2020) 482

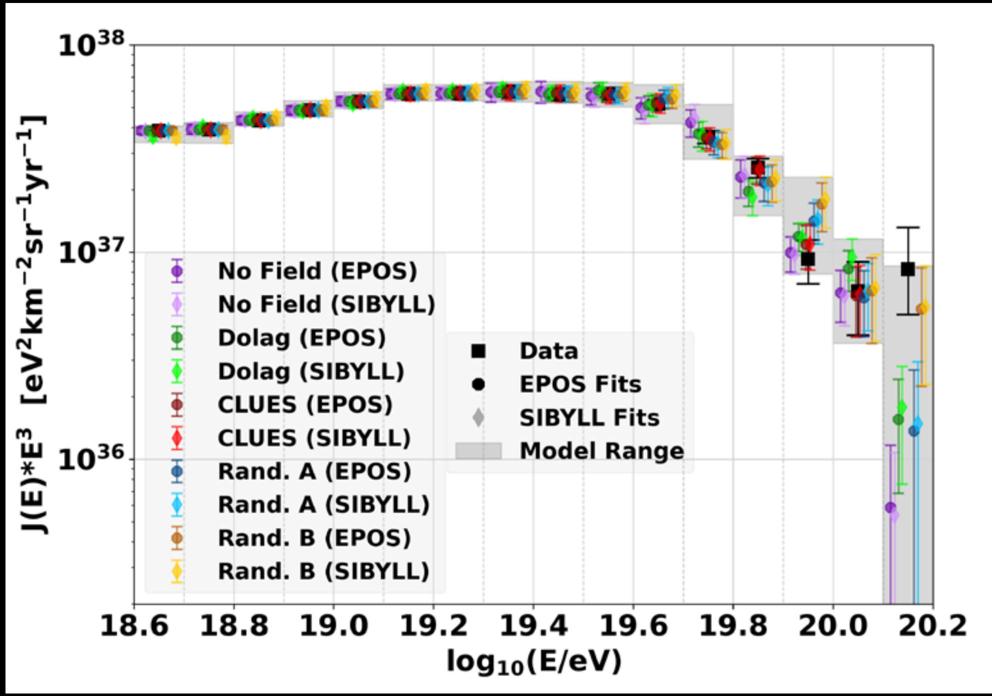

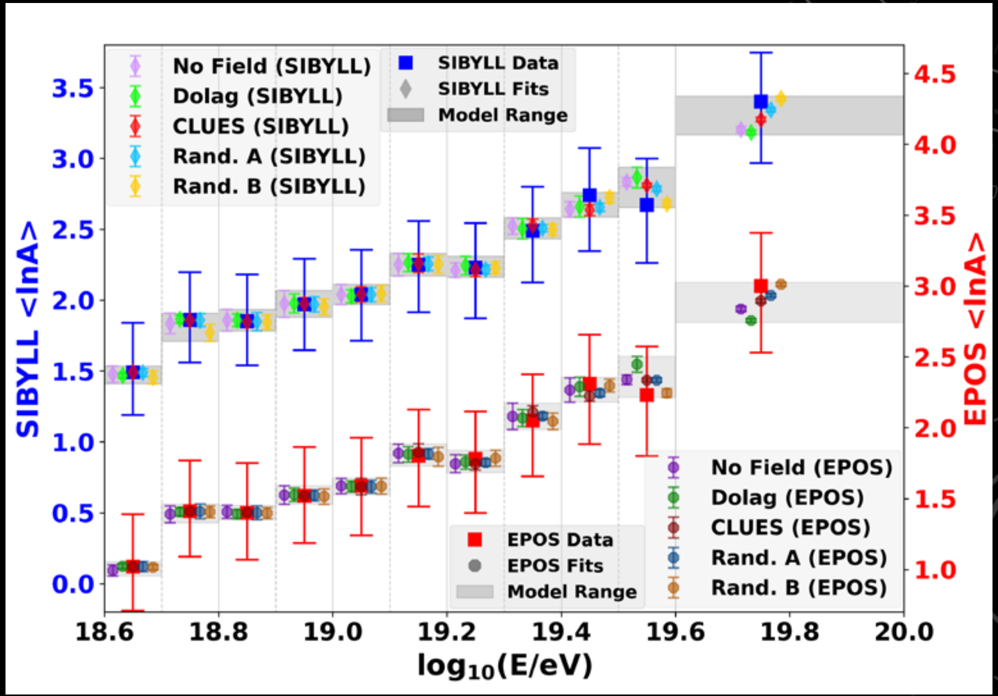

- Energy Spectra for all models.
- Highest energy bin generally not fit.
  - FR0 perhaps not expected as a significant contributor.

- ⟨lnA⟩ for all models.
- Very good fit. (44 parameters…)

MEAN LOG MASS <lnA> FITS (EVOLVING FRACTIONS)

Data From: Yushkov, A. et al., Mass Composition of Cosmic Rays with Energies above $10^{17.2}$ eV from the Hybrid Data of the Pierre Auger Observatory, *PoS* ICRC2019 (2020) 482

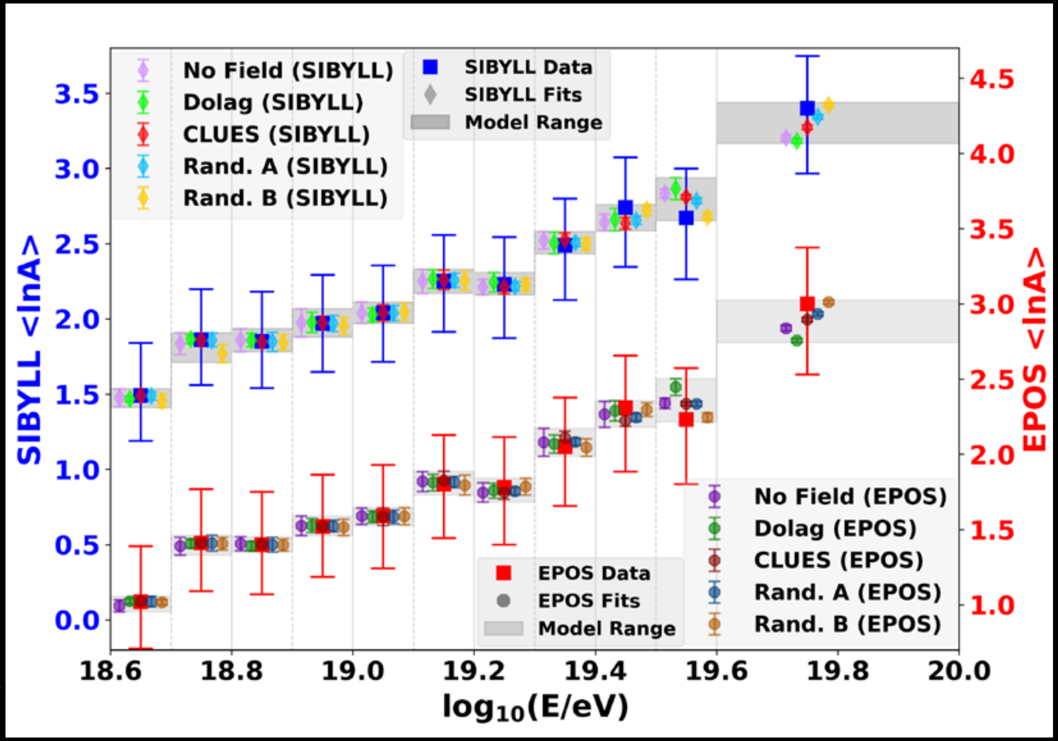

⟨lnA⟩ for all models

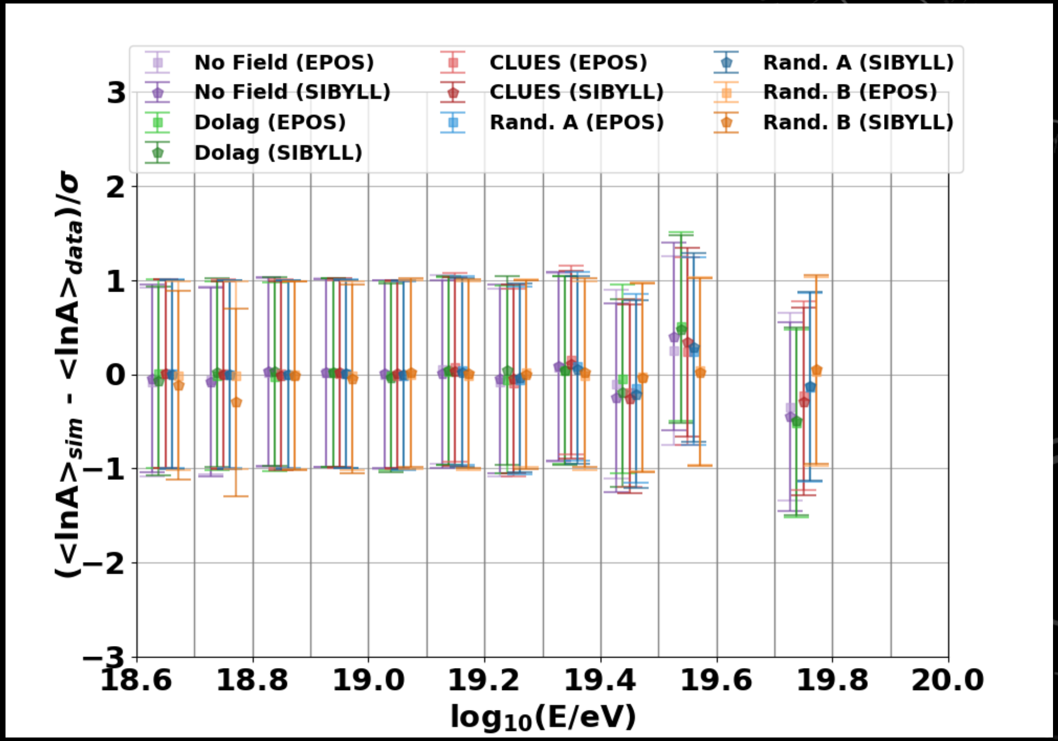

⟨lnA⟩ Residuals for all models

FIT PARAMETER RESULTS VS MAGNETIC FIELD

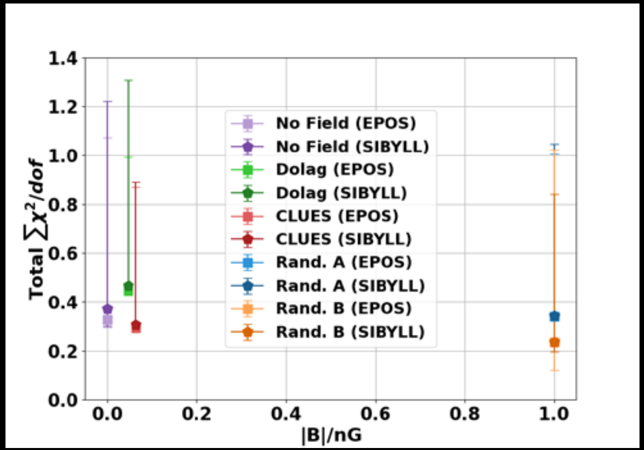

Goodness-of-fit

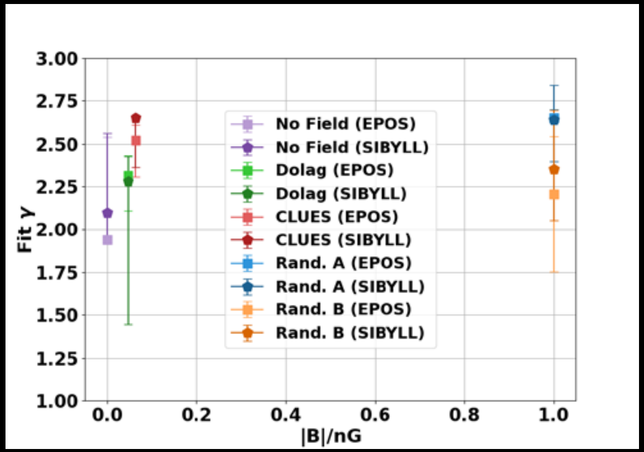

Power law Spectral Index γ

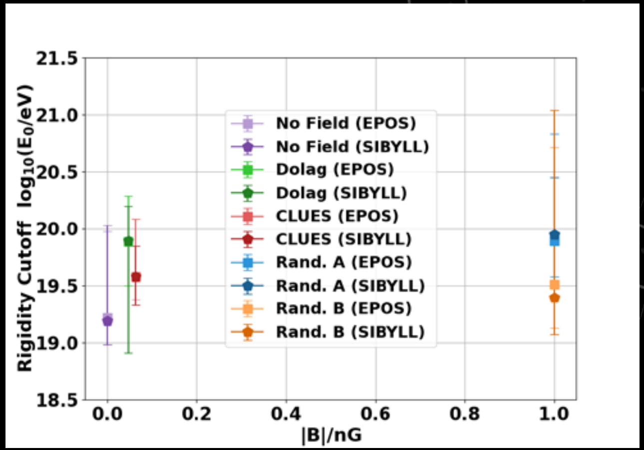

Rigidity cutoff R_{cut}

Error bars: 1 Gaussian σ C.I. around best fit for bootstrapped sims & Gaussian sampled data.

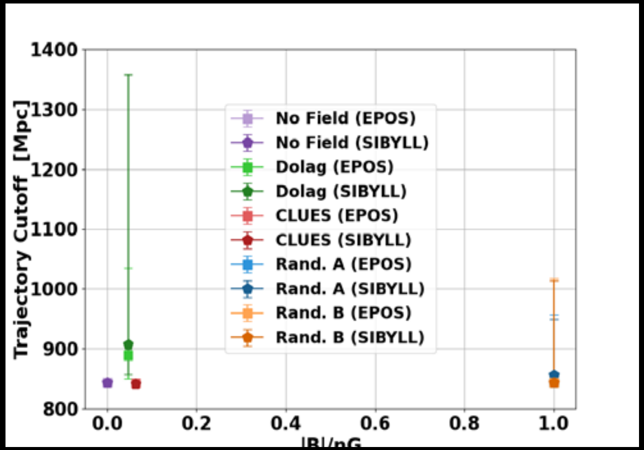

Trajectory cutoff D_{cut}

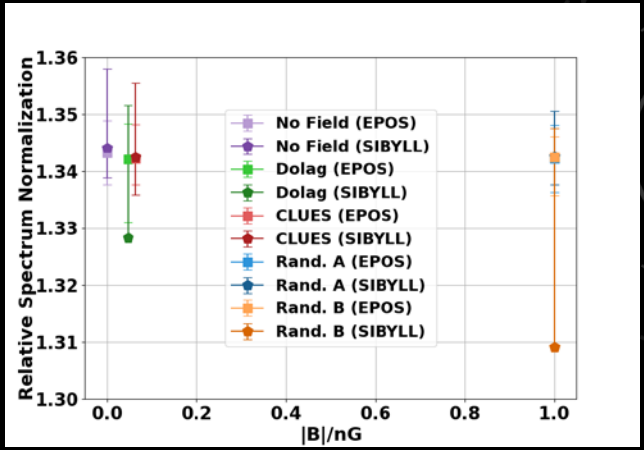

Spectrum Normalization

EVOLVING NUCLEI FRACTIONS (EMITTED)

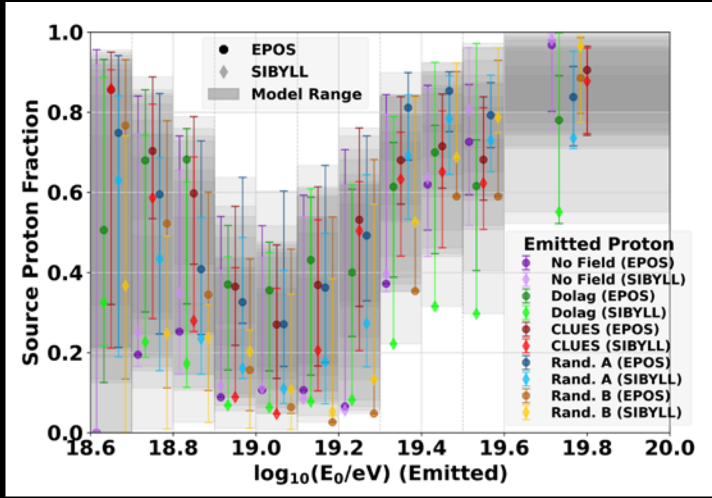

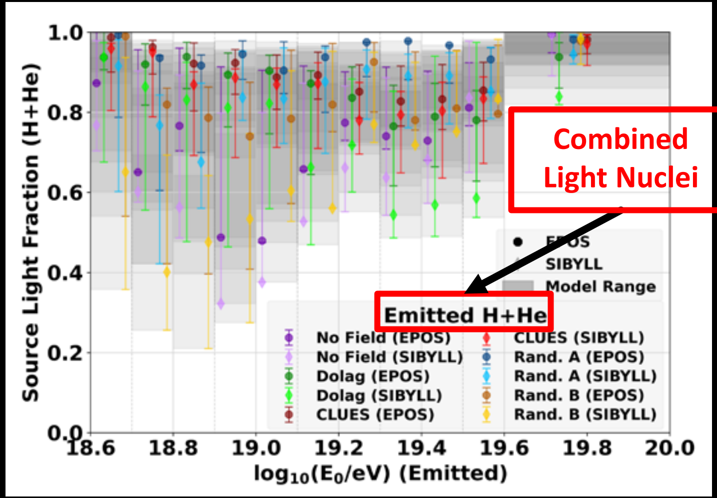

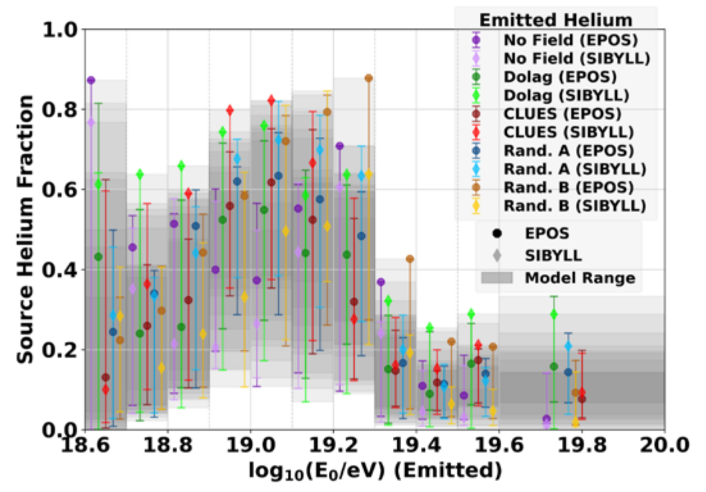

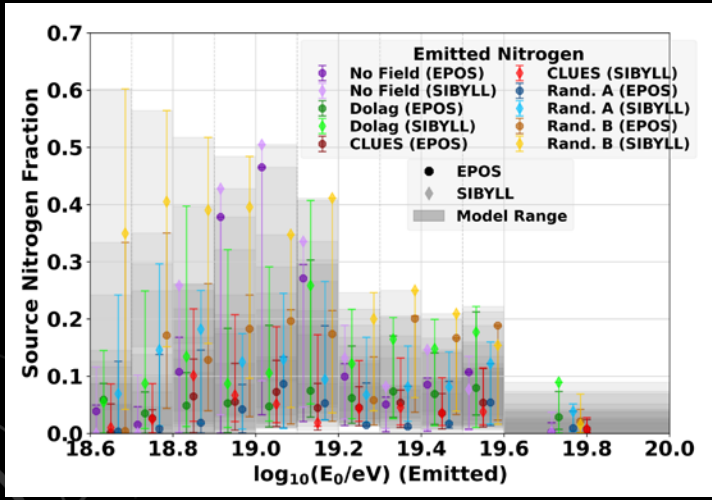

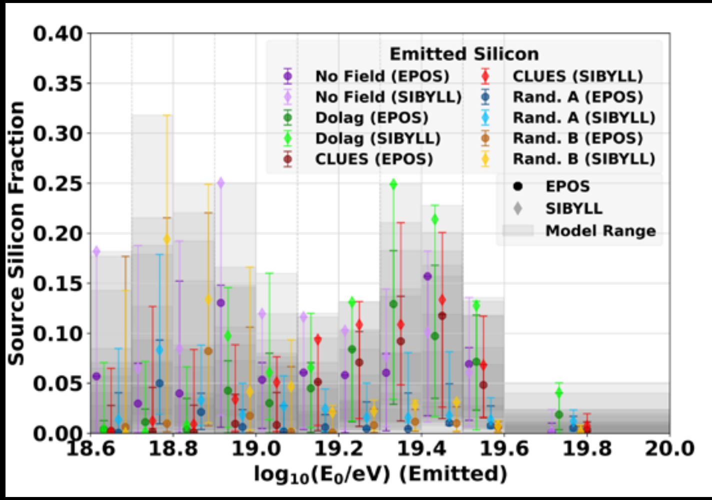

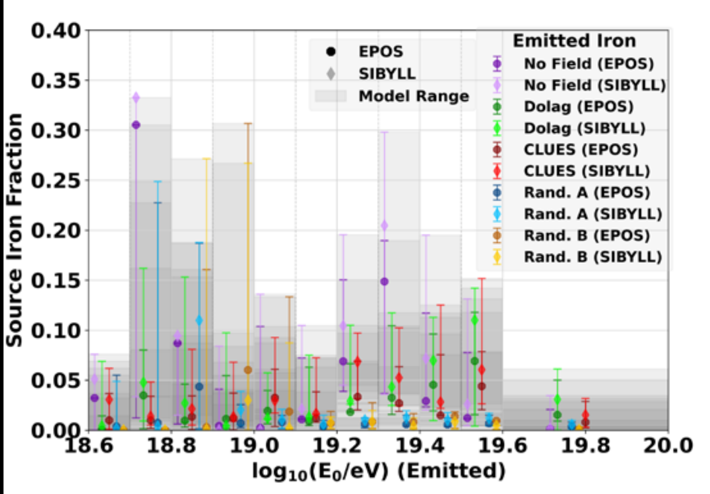

Emitted Nuclei Fraction Versus Magnetic Field

PHOTONS – (RAND.B–SIBYLL CONFIGURATION)

RAND.B–SIBYLL

Red/green areas are no magnetic field and GZK only.

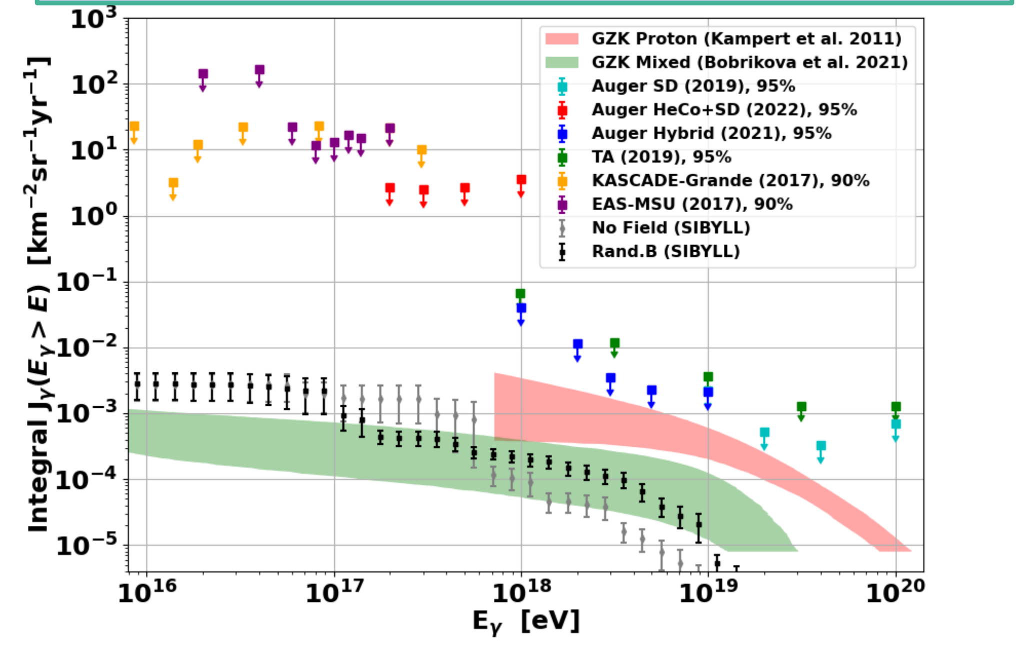

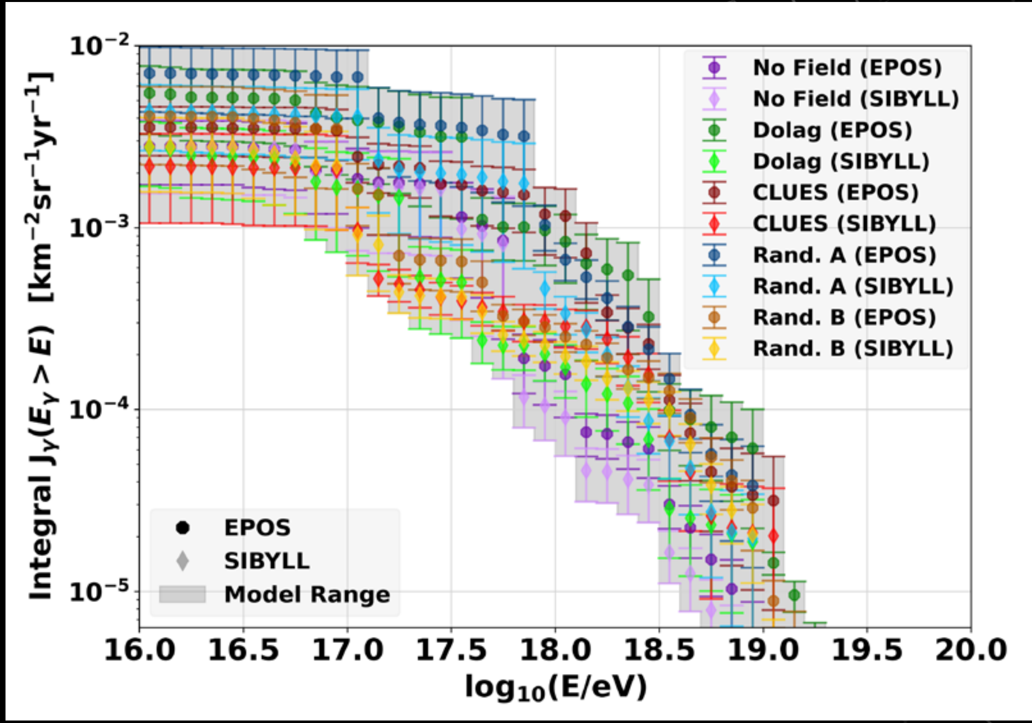

"A Search for Photons with Energies Above 2×10^17 eV Using Hybrid Data from the Low-Energy Extensions of the Pierre Auger Observatory"
P. Abreu et al 2022 ApJ 933 125
arXiv:2205.14864

Integral photon flux for all models

NEUTRINOS – (RAND.B–SIBYLL CONFIGURATION)

RAND.B–SIBYLL

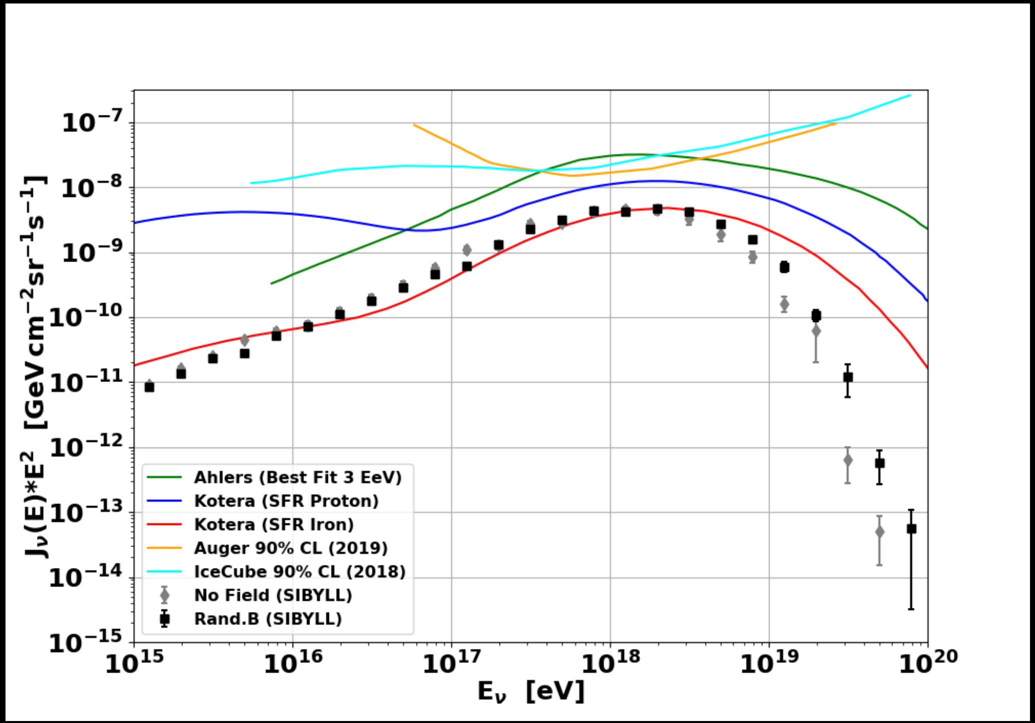

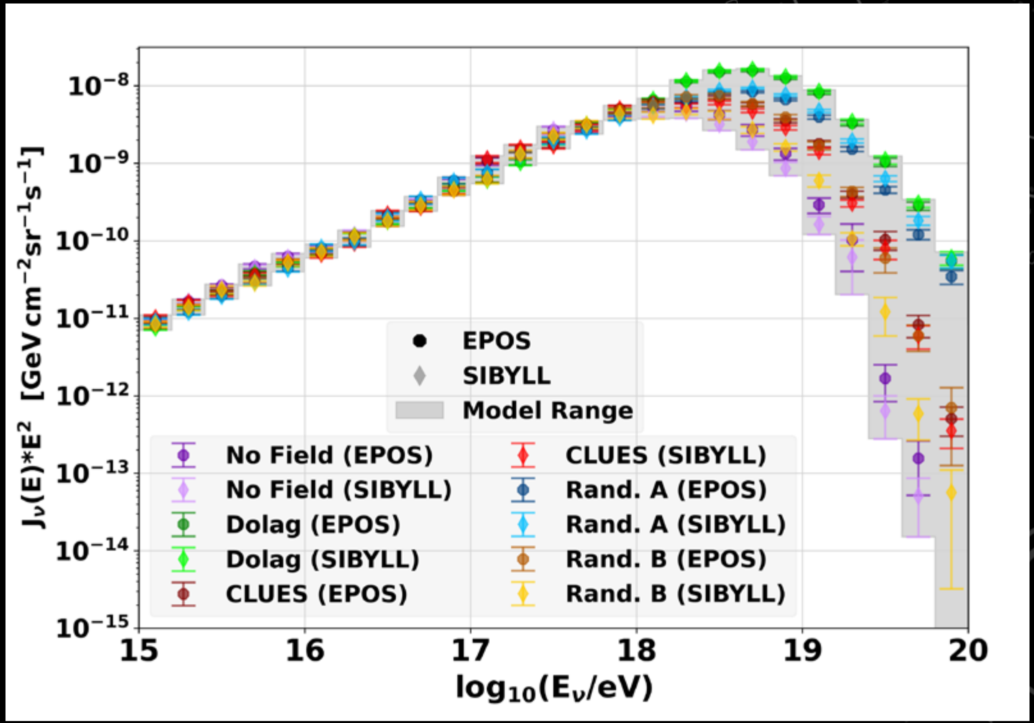

Kotera et al: JCAP (2010) arXiv:1009.1382
Ahlers et al: Astropart.Phys.(2010) arXiv:1005.2620v2
IceCube: Phys.Rev.D(2018) arXiv:1807.01820v2
Auger: JCAP10 (2019) arXiv:1906.07422v2

Neutrino flux for all models

EVOLVING FRACTION CONCLUSIONS

Best Fit: Rand.B 1 nG ($\langle l_{\mathrm{corr}} \rangle = 647$ kpc) with SIBYLL EAS model.

- Next best: Rand.B field with EPOS EAS model.
- Generally EPOS is the best fit – third: CLUES-EPOS, fourth: CLUES-SIBYLL

General trends with increasing magnetic field strength:

- Increases: γ
- Rather stable: R_{cut}

General trends with increasing energy:

- Increases: Proton emission.
- Rather stable: Light emission.
- Decreases: Heavy emission.

Extremely good fits (high parameters) still may require another source type at highest energies.

Photon spectra: consistent with mixed composition from GZK only ($\mathbf{E} > \sim 10^{17}$).

- Flux increases with magnetic fields.
- Below experimental limits.

Neutrino spectra: lower flux than expected from Kotera model for mixed composition.

- Flux increases with magnetic fields.
- Below experimental limits.

APPENDIX

CONSTANT FRACTION ADDITIONAL

INTERGALACTIC PROPAGATION

CRPropa 3 used to simulate propagation of five nuclei (proton, helium, nitrogen, silicon, and iron) UHECR primaries through the intergalactic medium.

Interactions with the CMB, IRB, and URB include:

- **Photo-pion production (GZK effect).**
- **Pair-production (including double and triple).**
- **Inverse Compton scattering.**

General interactions include:

- **Redshift adiabatic cooling.**
- **Nuclear decay.**

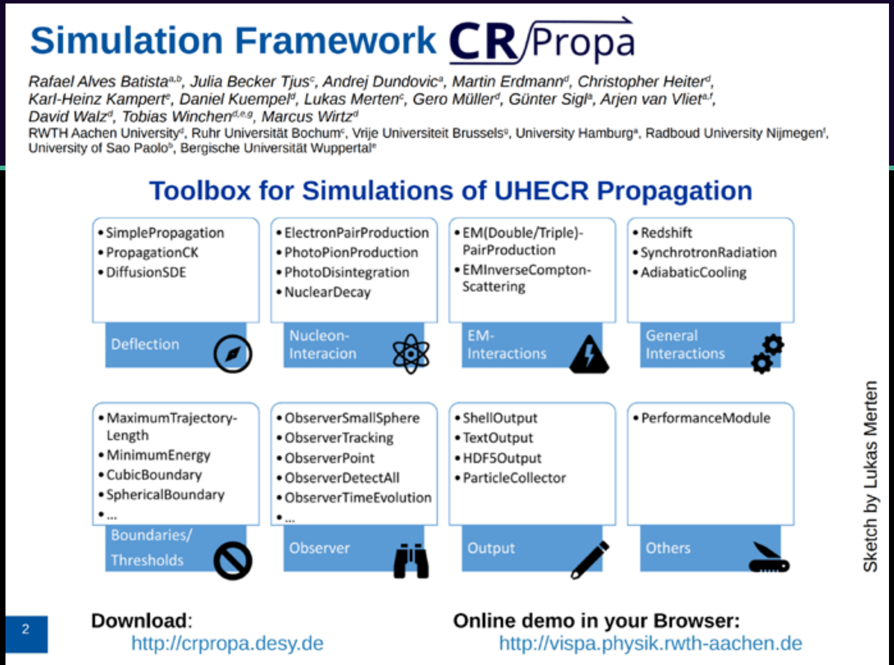

VARIANCE RESULTS

- Var(lnA) for log10(E) from 18.6 to 19.0
  - No field-Sibyll: 3.38 ± 0.04
  - No field-EPOS: 3.36 ± 0.07
  - No field-QGS4: 2.49 ± 0.12
  - Dolag-Sibyll: 2.52 ± 0.06
  - Dolag-EPOS: 2.21 ± 0.08
  - Dolag-QGS4: 1.71 ± 0.06
  - CLUES-Sibyll: 3.29 ± 0.06
  - CLUES-EPOS: 2.66 ± 0.10
  - CLUES-QGS4: 1.70 ± 0.09
  - 1ng1mpc-Sibyll: 1.19 ± 0.04
  - 1ng1mpc-EPOS: 1.16 ± 0.05
  - 1ng1mpc-QGS4: 0.66 ± 0.04
  - 1ng3mpc-Sibyll: 1.23 ± 0.02
  - 1ng3mpc-EPOS: 1.22 ± 0.02
  - 1ng3mpc-QGS4: 0.62 ± 0.01

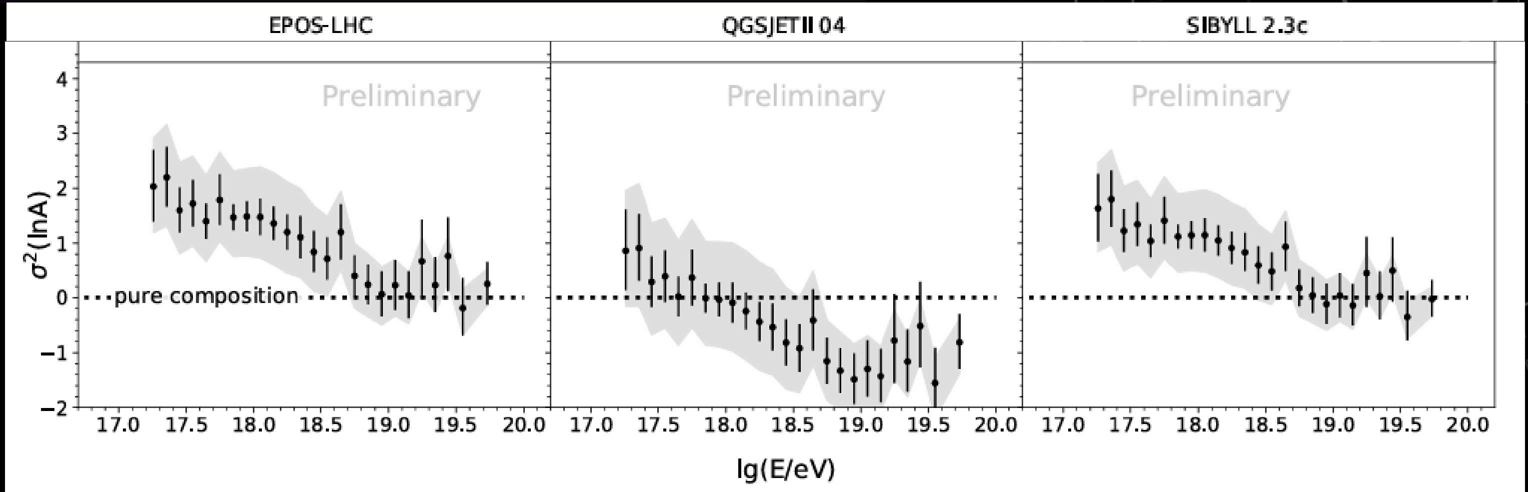

Data for log10(E) from 18.5 to 19.0:
1.64 ± 0.92

Does not include muon uncertainty

Yushkov, A. 2020, PoS, ICRC2019, 482

ADDING Var(lnA)

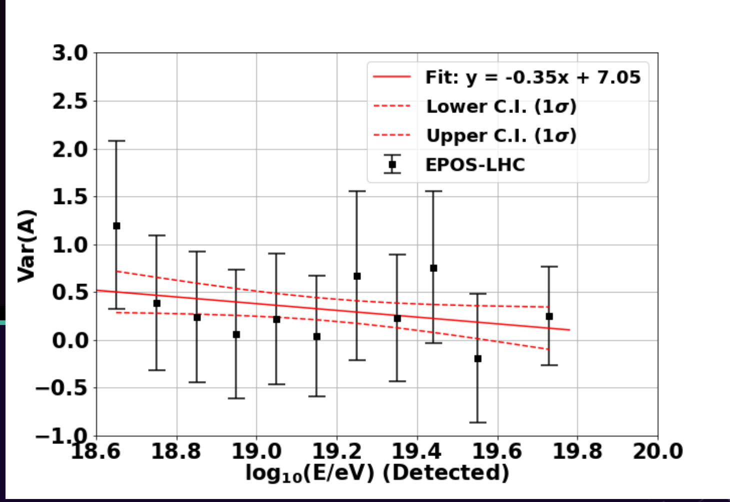

- *EPOS-LHC* $Var(lnA)$
  - *Negative variances not calculable.*
  - Slope -0.29 +/- 0.30
    - *Not significant with uncertainties in* A *transform.*
    - *Transforming* A *to* $X_{\max}$ *transfers uncertainty to simulation.*

- *Adding more rigid constraint* than $Var(lnA)$ χ^2:
  - *Constrain simulation variance slope +/- 1σ.*
    - χ^2 : 2.67 to 7.45
    - Gamma γ: 2.67 to 3.14
    - Rigidity cutoff: 37×10^{18} to 21×10^{18}
    - Trajectory cutoff: 424 Mpc to 225 Mpc
    - Observed nuclei fractions:
      - Proton: 34% to 52%
      - Helium: 27% to 0%
      - H+He: 61% to 52%
      - Nitrogen: 25% to 34%
      - Silicon: 6% to 8.3%
      - Iron: 7% to 5.4%

z<0.05

- *1 nG 234 kpc magnetic field*

FIT RESULT TABLES

Field	Model	$\Sigma\chi^2/\text{dof}$	γ	$\log_{10}(R_{cut}/V)$	D_{cut}/Mpc	n
No Field	SIBYLL	3.21	$2.51^{+0.02}_{-0.67}$	$19.36^{+0.23}_{-0.31}$	843^{+0}_{-1}	$1.337^{+0.016}_{-0.003}$
	EPOS	3.15	$2.50^{+0.02}_{-0.16}$	$19.40^{+0.13}_{-0.06}$	843^{+0}_{-0}	$1.337^{+0.011}_{-0.004}$
	QGS4	3.47	$2.47^{+0.03}_{-0.08}$	$19.43^{+0.10}_{-0.03}$	843^{+0}_{-0}	$1.338^{+0.006}_{-0.006}$
Dolag	SIBYLL	4.41	$2.29^{+0.06}_{-0.79}$	$19.74^{+0.00}_{-0.40}$	890^{+320}_{-41}	$1.341^{+0.008}_{-0.008}$
	EPOS	4.74	$2.23^{+0.11}_{-0.06}$	$19.75^{+0.03}_{-0.29}$	889^{+230}_{-41}	$1.339^{+0.007}_{-0.007}$
	QGS4	6.28	$2.23^{+0.08}_{-0.09}$	$19.64^{+0.10}_{-0.12}$	890^{+47}_{-42}	$1.335^{+0.005}_{-0.008}$
CLUES	SIBYLL	1.76	$2.54^{+0.00}_{-0.19}$	$19.45^{+0.50}_{-0.12}$	842^{+0}_{-0}	$1.354^{+0.006}_{-0.015}$
	EPOS	1.87	$2.43^{+0.06}_{-0.13}$	$19.51^{+0.36}_{-0.07}$	842^{+0}_{-1}	$1.347^{+0.006}_{-0.011}$
	QGS4	3.10	$2.32^{+0.08}_{-0.05}$	$19.56^{+0.08}_{-0.07}$	841^{+1}_{-0}	$1.334^{+0.006}_{-0.007}$
Rand.A	SIBYLL	2.84	$2.40^{+0.07}_{-0.11}$	$19.86^{+0.12}_{-0.18}$	843^{+80}_{-0}	$1.342^{+0.007}_{-0.005}$
	EPOS	2.15	$2.34^{+0.08}_{-0.09}$	$19.69^{+0.19}_{-0.08}$	843^{+76}_{-0}	$1.341^{+0.006}_{-0.004}$
	QGS4	2.51	$2.23^{+0.07}_{-0.07}$	$19.58^{+0.07}_{-0.08}$	846^{+69}_{-0}	$1.341^{+0.005}_{-0.006}$
Rand.B	SIBYLL	2.57	$2.47^{+0.04}_{-0.16}$	$19.71^{+1.40}_{-0.08}$	843^{+156}_{-0}	$1.346^{+0.009}_{-0.006}$
	EPOS	2.29	$2.33^{+0.09}_{-0.15}$	$19.60^{+0.23}_{-0.09}$	843^{+140}_{-0}	$1.346^{+0.005}_{-0.006}$
	QGS4	2.60	$1.97^{+0.26}_{-0.05}$	$19.52^{+0.08}_{-0.07}$	854^{+66}_{-11}	$1.343^{+0.006}_{-0.004}$

Table 1: The FR0 combined fit results total sum chi-square per degree of freedom, spectral index γ, exponential rigidity cutoff ($\log_{10}(R_{cut})$), trajectory cutoff (D_{cut}), and spectrum normalization for all 15 models. The three extensive air-shower models are EPOS-LHC (EPOS), Sibyll2.3c (SIBYLL), and QGSJetII-04 (QGS4).

FIT RESULT TABLES

Field	Model	$f_{H}(\%) + f_{He}(\%)$	$f_{H}(\%)$	$f_{He}(\%)$	$f_{N}(\%)$	$f_{Si}(\%)$	$f_{Fe}(\%)$
No Field	SIBYLL	$88.7^{+0.2}_{-24.0}$	$88.7^{+0.1}_{-88.7}$	$0.0^{+16.5}_{-0.0}$	$0.0^{+23.1}_{-0.0}$	$6.1^{+6.8}_{-2.3}$	$5.2^{+2.0}_{-4.0}$
	EPOS	$93.4^{+0.7}_{-7.2}$	$93.4^{+0.6}_{-16.5}$	$0.0^{+12.1}_{-0.0}$	$0.0^{+5.8}_{-0.0}$	$2.9^{+2.4}_{-1.8}$	$3.7^{+0.8}_{-0.8}$
	QGS4	$97.6^{+0.3}_{-1.1}$	$97.6^{+0.1}_{-8.8}$	$0.0^{+7.8}_{-0.0}$	$0.0^{+0.0}_{-0.0}$	$0.2^{+1.2}_{-0.2}$	$2.2^{+0.2}_{-0.5}$
Dolag	SIBYLL	$84.3^{+5.2}_{-11.9}$	$0.0^{+85.6}_{-0.0}$	$84.3^{+0.0}_{-84.3}$	$0.0^{+16.6}_{-0.0}$	$2.5^{+10.5}_{-2.4}$	$13.2^{+0.0}_{-12.1}$
	EPOS	$90.8^{+3.7}_{-3.8}$	$0.0^{+87.9}_{-0.0}$	$90.8^{+0.0}_{-90.0}$	$0.0^{+0.0}_{-0.0}$	$0.0^{+5.8}_{-0.0}$	$9.2^{+0.0}_{-5.2}$
	QGS4	$97.1^{+0.4}_{-1.0}$	$54.4^{+28.3}_{-35.4}$	$42.7^{+34.7}_{-28.4}$	$0.0^{+0.0}_{-0.0}$	$0.0^{+0.0}_{-0.0}$	$2.9^{+0.9}_{-0.5}$
CLUES	SIBYLL	$91.8^{+0.3}_{-11.4}$	$74.5^{+8.5}_{-74.5}$	$17.3^{+66.2}_{-10.8}$	$0.0^{+0.0}_{-0.0}$	$0.0^{+9.2}_{-0.0}$	$8.2^{+3.5}_{-1.8}$
	EPOS	$94.4^{+0.4}_{-4.4}$	$68.6^{+14.1}_{-68.6}$	$25.8^{+64.4}_{-13.4}$	$0.0^{+0.0}_{-0.0}$	$0.0^{+3.5}_{-0.0}$	$5.6^{+2.5}_{-0.9}$
	QGS4	$97.4^{+0.4}_{-0.5}$	$68.8^{+16.3}_{-15.8}$	$28.6^{+15.6}_{-16.1}$	$0.0^{+0.0}_{-0.0}$	$0.0^{+0.0}_{-0.0}$	$2.6^{+0.5}_{-0.4}$
Rand.A	SIBYLL	$69.3^{+11.1}_{-19.2}$	$0.0^{+43.1}_{-0.0}$	$69.3^{+8.3}_{-54.4}$	$24.5^{+19.2}_{-12.3}$	$1.3^{+3.0}_{-1.3}$	$4.9^{+1.0}_{-1.4}$
	EPOS	$87.6^{+5.6}_{-4.2}$	$38.0^{+23.3}_{-38.0}$	$49.6^{+34.2}_{-23.5}$	$9.5^{+3.5}_{-7.3}$	$0.3^{+1.8}_{-0.3}$	$2.6^{+0.9}_{-0.5}$
	QGS4	$98.9^{+0.0}_{-3.5}$	$57.9^{+18.4}_{-12.1}$	$41.0^{+10.0}_{-20.7}$	$0.0^{+3.5}_{-0.0}$	$0.0^{+0.1}_{-0.0}$	$1.1^{+0.2}_{-0.2}$
Rand.B	SIBYLL	$58.4^{+10.5}_{-23.6}$	$48.3^{+5.3}_{-48.3}$	$10.1^{+41.8}_{-10.1}$	$38.8^{+22.2}_{-13.4}$	$0.0^{+3.5}_{-0.0}$	$2.8^{+1.6}_{-0.4}$
	EPOS	$79.5^{+5.8}_{-6.5}$	$57.7^{+20.2}_{-37.2}$	$21.8^{+34.9}_{-21.8}$	$18.2^{+5.8}_{-6.3}$	$0.7^{+1.9}_{-0.7}$	$1.6^{+0.7}_{-0.4}$
	QGS4	$95.8^{+1.7}_{-4.5}$	$45.6^{+41.0}_{-9.4}$	$50.2^{+9.0}_{-43.1}$	$2.2^{+5.1}_{-2.2}$	$0.9^{+0.6}_{-0.9}$	$1.1^{+0.2}_{-0.4}$

Table 3: The FR0 combined fit nuclei emission percentages for proton, helium, nitrogen, silicon, and iron primaries for all 15 models.

FIT RESULT TABLES

Table 2. Constant Fraction Bootstrap Energy Spectrum Parameters

Field	Model	$\Sigma\chi^2$/dof	γ	$\log_{10}(R_{cut}/V)$	D_{cut}/Mpc	n
No Field	SIBYLL	3.21	$2.48^{+0.27}_{-0.27}$	$19.38^{+0.23}_{-0.23}$	843^{+0}_{-0}	$1.341^{+0.006}_{-0.006}$
	EPOS	3.15	$2.48^{+0.26}_{-0.26}$	$19.40^{+0.13}_{-0.13}$	843^{+0}_{-0}	$1.338^{+0.005}_{-0.005}$
	QGS4	3.47	$2.45^{+0.04}_{-0.04}$	$19.43^{+0.06}_{-0.06}$	843^{+0}_{-0}	$1.335^{+0.004}_{-0.004}$
Dolag	SIBYLL	4.41	$2.07^{+0.23}_{-0.23}$	$19.04^{+0.57}_{-0.57}$	871^{+126}_{-29}	$1.339^{+0.005}_{-0.005}$
	EPOS	4.74	$2.33^{+0.38}_{-0.38}$	$19.37^{+0.24}_{-0.24}$	864^{+180}_{-22}	$1.334^{+0.004}_{-0.004}$
	QGS4	6.28	$2.24^{+0.37}_{-0.37}$	$19.64^{+0.07}_{-0.07}$	893^{+86}_{-51}	$1.335^{+0.004}_{-0.004}$
CLUES	SIBYLL	1.76	$2.54^{+0.15}_{-0.15}$	$19.41^{+0.34}_{-0.34}$	842^{+0}_{-0}	$1.352^{+0.007}_{-0.007}$
	EPOS	1.87	$2.41^{+0.07}_{-0.07}$	$19.51^{+0.15}_{-0.15}$	842_0^{+0}	$1.346^{+0.005}_{-0.005}$
	QGS4	3.10	$2.31^{+0.05}_{-0.05}$	$19.56^{+0.06}_{-0.06}$	842^{+0}_{-0}	$1.337^{+0.004}_{-0.004}$
Rand.A	SIBYLL	2.84	$2.36^{+0.26}_{-0.26}$	$19.87^{+1.66}_{-1.66}$	864^{+81}_{-22}	$1.343^{+0.001}_{-0.001}$
	EPOS	2.15	$2.31^{+0.05}_{-0.05}$	$19.67^{+0.11}_{-0.11}$	853^{+36}_{-11}	$1.343^{+0.003}_{-0.003}$
	QGS4	2.51	$2.25^{+0.07}_{-0.07}$	$19.59^{+0.08}_{-0.08}$	854^{+29}_{-12}	$1.342^{+0.004}_{-0.004}$
Rand.B	SIBYLL	2.57	$2.43^{+0.06}_{-0.06}$	$19.70^{+10.20}_{-10.20}$	852^{+53}_{-10}	$1.347^{+0.005}_{-0.005}$
	EPOS	2.29	$2.36^{+0.10}_{-0.10}$	$19.54^{+7.2}_{-7.2}$	854^{+64}_{-12}	$1.346^{+0.000}_{-0.000}$
	QGS4	2.60	$2.15^{+0.14}_{-0.14}$	$19.45^{+0.62}_{-0.62}$	848^{+48}_{-6}	$1.342^{+0.003}_{-0.003}$

Notes. The FR0 constant fraction combined fit bootstrap distribution most probable spectral index γ, exponential rigidity cutoff ($\log_{10}(R_{cut}/V)$), trajectory cutoff (D_{cut}), and spectrum normalization for all 15 configurations.

FIT RESULT TABLES

Table 4. Constant Fraction Bootstrap Composition Parameters

Field	Model	$f_H(\%) + f_{He}(\%)$	$f_H(\%)$	$f_{He}(\%)$	$f_N(\%)$	$f_{Si}(\%)$	$f_{Fe}(\%)$
No Field	SIBYLL	$86.3^{+13.7}_{-15.6}$	$85.6^{+14.4}_{-21.7}$	$0.6^{+15.2}_{-0.6}$	$2.8^{+15.8}_{-2.8}$	$5.6^{+3.1}_{-3.1}$	$5.4^{+2.3}_{-2.3}$
	EPOS	$92.8^{+5.3}_{-5.3}$	$91.4^{+8.6}_{-13.2}$	$1.4^{+10.7}_{-1.4}$	$0.6^{+5.3}_{-0.6}$	$2.9^{+1.5}_{-1.5}$	$3.7^{+0.8}_{-0.8}$
	QGS4	$97.6^{+0.8}_{-0.8}$	$96.4^{+3.6}_{-7.6}$	$1.2^{+7.4}_{-1.2}$	$0.0^{+0.8}_{-0.0}$	$0.2^{+0.5}_{-0.2}$	$2.2^{+0.2}_{-0.2}$
Dolag	SIBYLL	$85.2^{+8.0}_{-8.0}$	$84.4^{+15.6}_{-22.6}$	$0.9^{+22.1}_{-0.9}$	$0.0^{+7.6}_{-0.0}$	$13.0^{+3.9}_{-3.9}$	$1.8^{+3.1}_{-1.8}$
	EPOS	$94.8^{+4.9}_{-4.9}$	$84.5^{+15.5}_{-23.6}$	$10.3^{+22.4}_{-10.3}$	$0.1^{+4.7}_{-0.1}$	$0.2^{+2.2}_{-0.2}$	$4.9^{+1.7}_{-1.7}$
	QGS4	$97.0^{+0.6}_{-0.6}$	$54.7^{+18.0}_{-18.0}$	$42.3^{+17.7}_{-17.7}$	$0.0^{+0.5}_{-0.0}$	$0.0^{+0.3}_{-0.0}$	$2.9^{+0.5}_{-0.5}$
CLUES	SIBYLL	$91.6^{+3.6}_{-3.6}$	$81.2^{+18.8}_{-23.3}$	$10.6^{+20.7}_{-10.6}$	$0.0^{+2.2}_{-0.0}$	$0.7^{+3.4}_{-0.7}$	$7.5^{+1.9}_{-1.9}$
	EPOS	$94.2^{+1.8}_{-1.8}$	$66.7^{+21.8}_{-21.8}$	$27.6^{+20.5}_{-20.5}$	$0.0^{+0.5}_{-0.0}$	$0.2^{+1.6}_{-0.2}$	$5.5^{+1.0}_{-1.0}$
	QGS4	$97.5^{+0.4}_{-0.4}$	$67.6^{+12.3}_{-12.3}$	$29.9^{+12.1}_{-12.1}$	$0.0^{+0.0}_{-0.0}$	$0.0^{+0.2}_{-0.0}$	$2.5^{+0.3}_{-0.3}$
Rand.A	SIBYLL	$70.0^{+11.4}_{-11.4}$	$5.3^{+14.7}_{-5.3}$	$63.9^{+17.5}_{-17.5}$	$25.1^{+11.8}_{-11.8}$	$0.7^{+1.5}_{-0.7}$	$5.0^{+0.9}_{-0.9}$
	EPOS	$87.6^{+4.6}_{-4.6}$	$36.2^{+15.9}_{-15.9}$	$51.5^{+16.0}_{-16.0}$	$9.5^{+4.9}_{-4.9}$	$0.2^{+0.8}_{-0.2}$	$2.7^{+0.5}_{-0.5}$
	QGS4	$98.4^{+1.1}_{-1.1}$	$60.6^{+10.1}_{-10.1}$	$37.7^{+10.4}_{-10.4}$	$0.5^{+1.2}_{-0.5}$	$0.0^{+0.2}_{-0.0}$	$1.1^{+0.2}_{-0.2}$
Rand.B	SIBYLL	$59.3^{+11.1}_{-11.1}$	$45.7^{+15.3}_{-15.3}$	$15.2^{+14.4}_{-14.4}$	$35.8^{+11.5}_{-11.5}$	$0.6^{+1.3}_{-0.6}$	$2.7^{+0.6}_{-0.6}$
	EPOS	$82.0^{+4.5}_{-4.5}$	$73.3^{+16.3}_{-16.3}$	$9.5^{+14.8}_{-9.5}$	$15.6^{+4.7}_{-4.7}$	$0.2^{+1.0}_{-0.2}$	$1.4^{+0.4}_{-0.4}$
	QGS4	$93.6^{+1.8}_{-1.8}$	$80.4^{+14.2}_{-14.2}$	$13.2^{+14.7}_{-13.2}$	$5.6^{+2.1}_{-2.1}$	$0.0^{+0.4}_{-0.0}$	$0.7^{+0.2}_{-0.2}$

Notes. The FR0 constant fraction combined fit bootstrap distribution most probable nuclei emission percentages for proton, helium, nitrogen, silicon, and iron primaries for all 15 configurations.

OBSERVED NUCLEI FRACTIONS

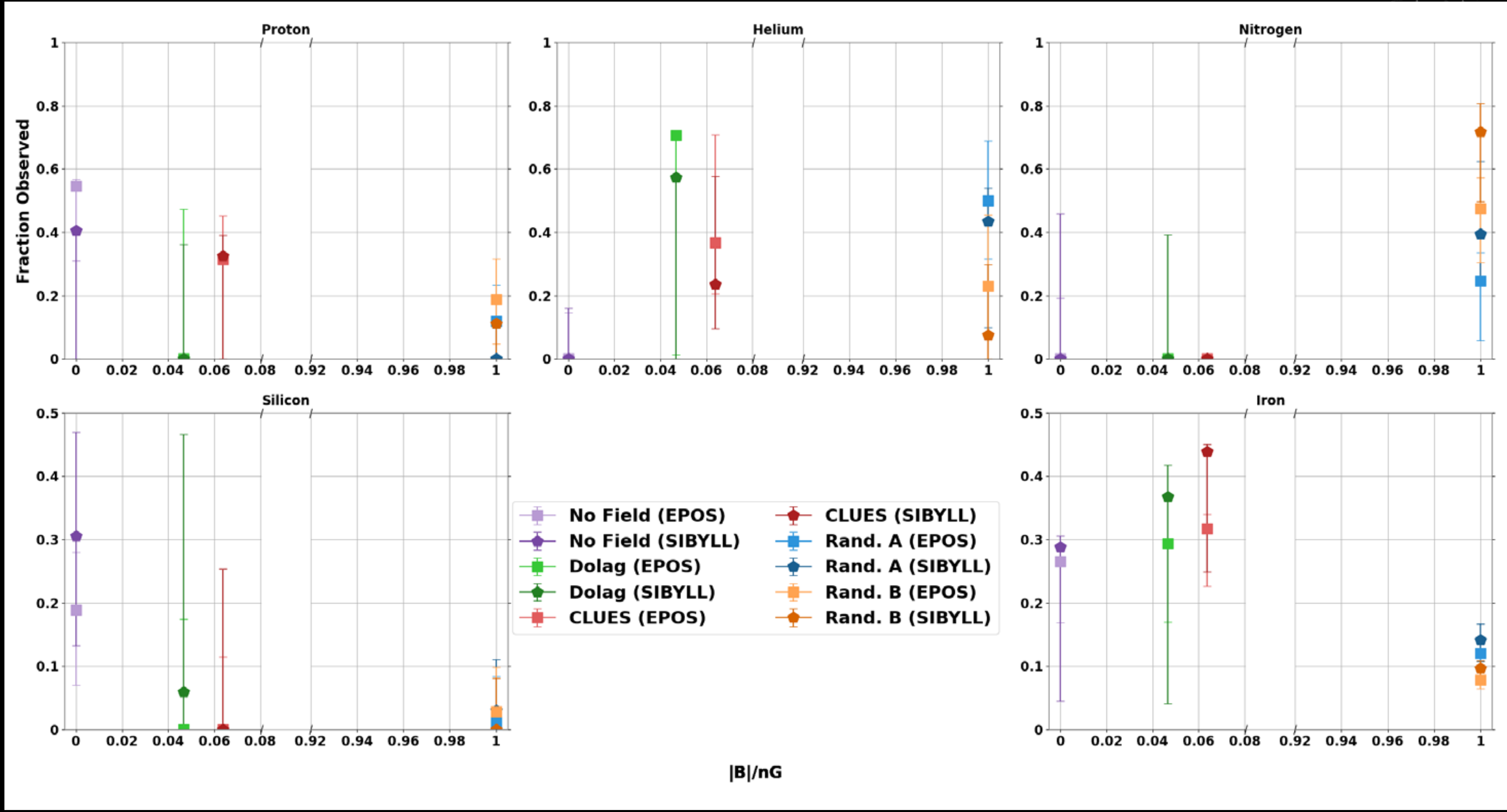

Observed Nuclei Fraction Versus Magnetic Field

SECONDARY RATIOS

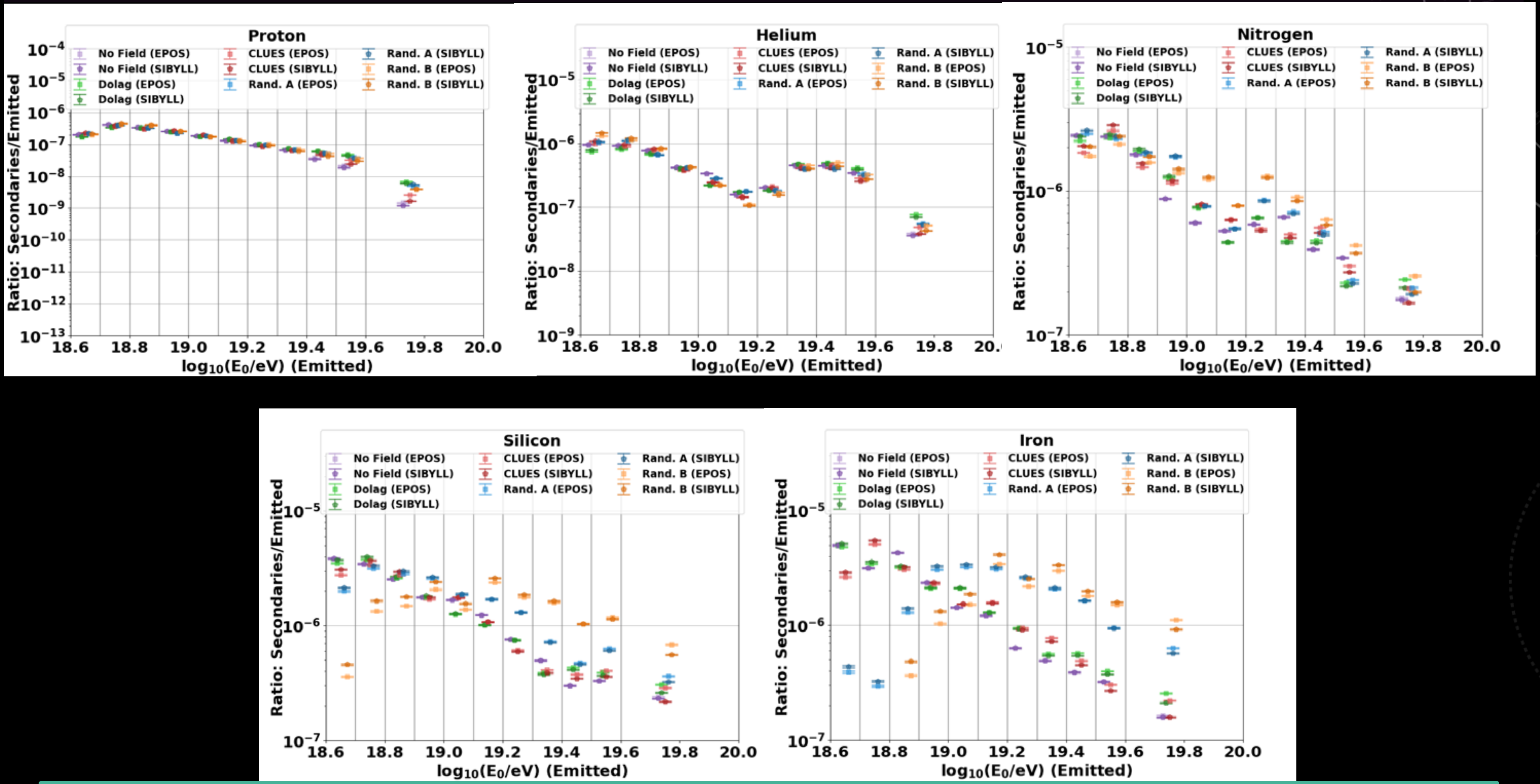

- Emitted energy binned ratios of observed secondaries to emitted nuclei.
- Total ratios used to convert constant observed fractions to emitted fraction.

FRACTIONS EMITTED

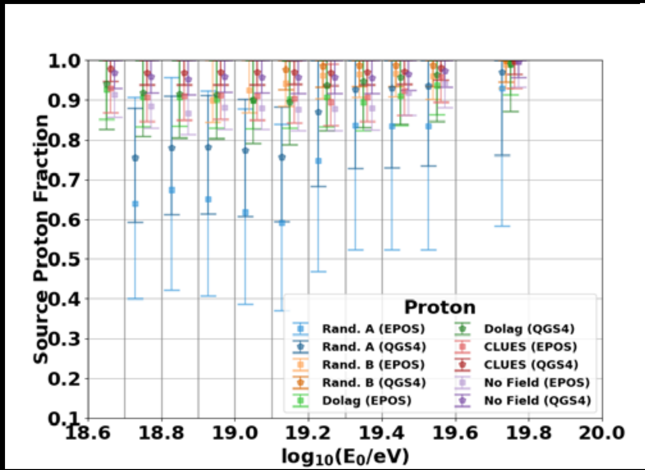

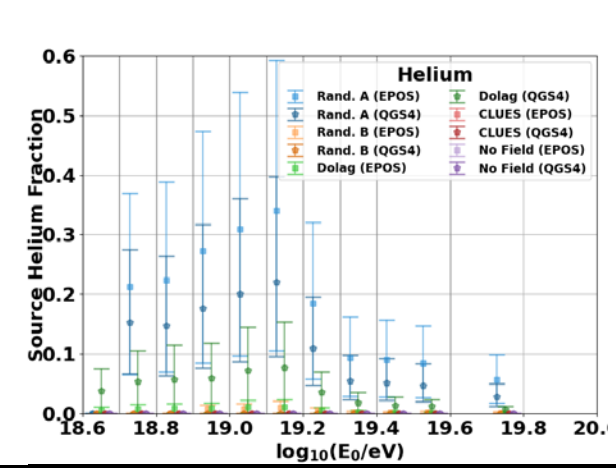

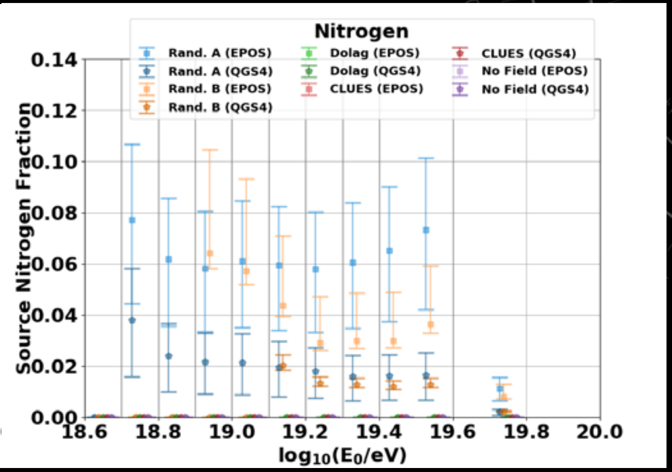

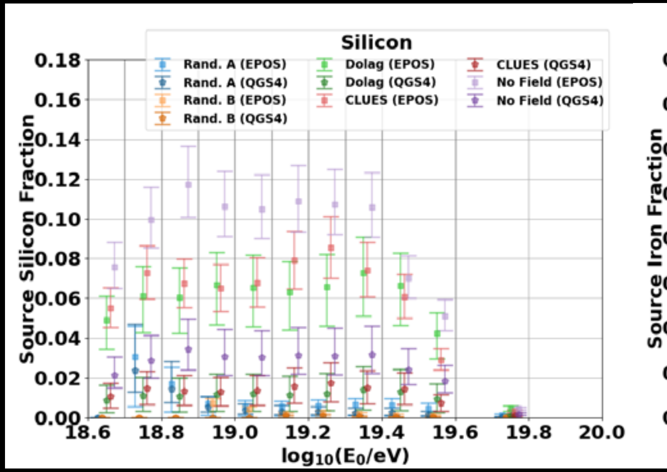

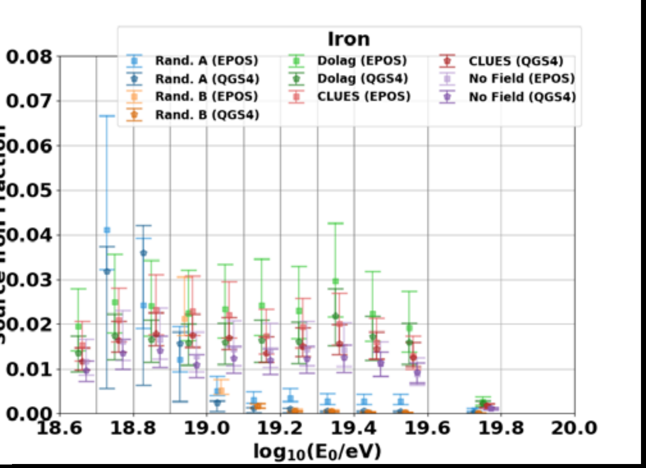

Emitted fractions in E_0 ins for observed constant fraction

OBSERVED <lnA>

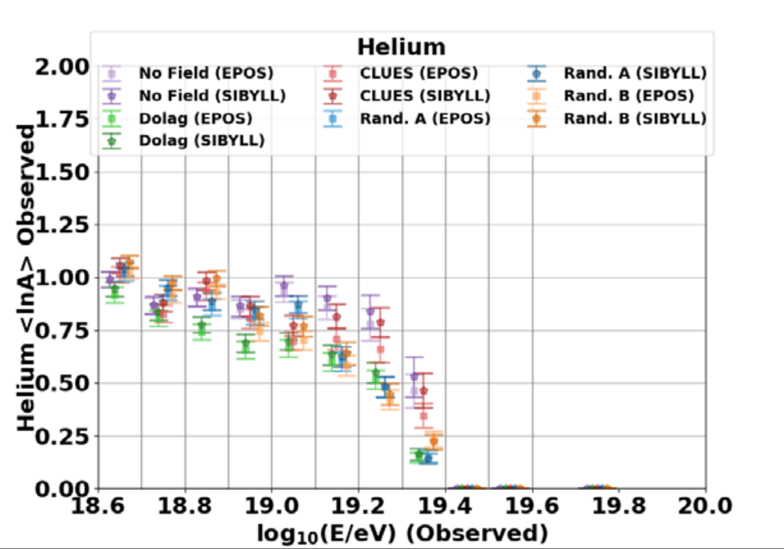

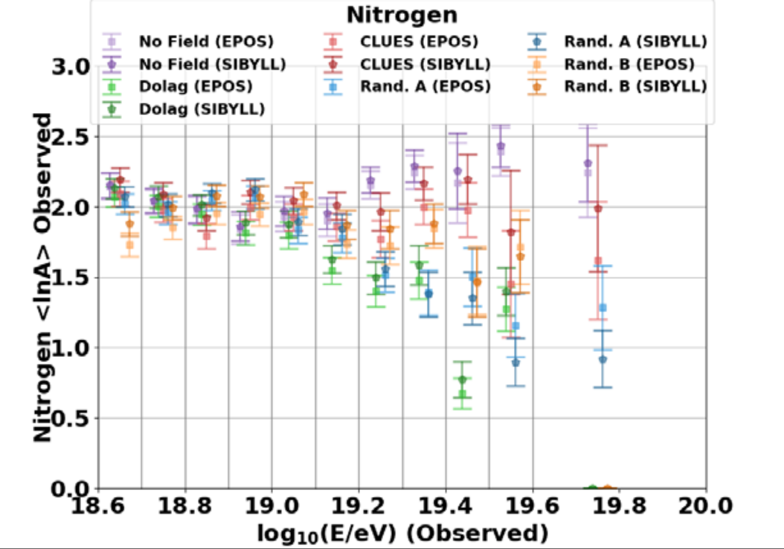

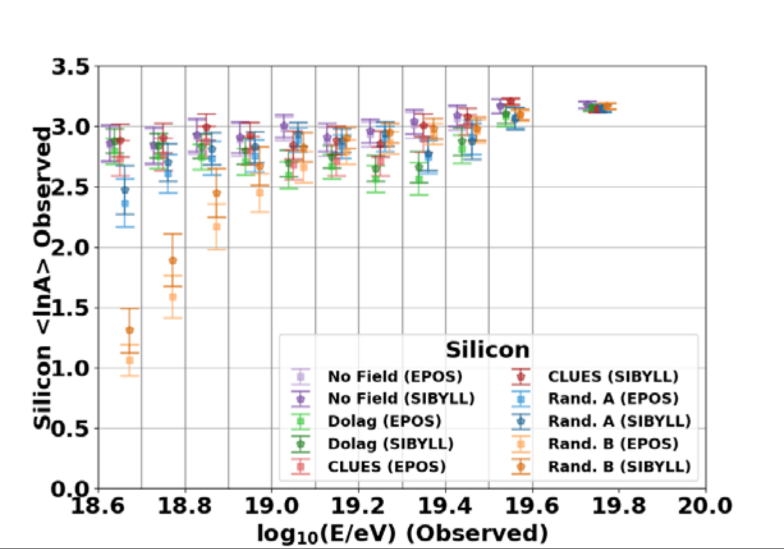

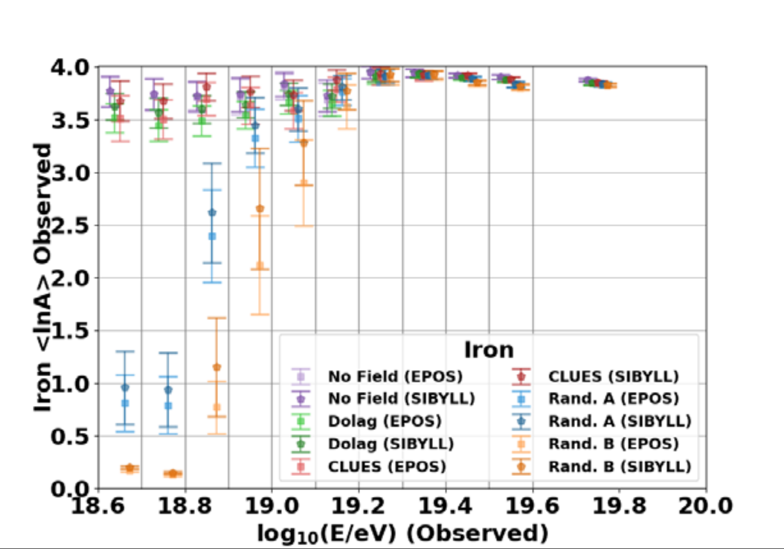

ENERGY SPECTRUM FITS

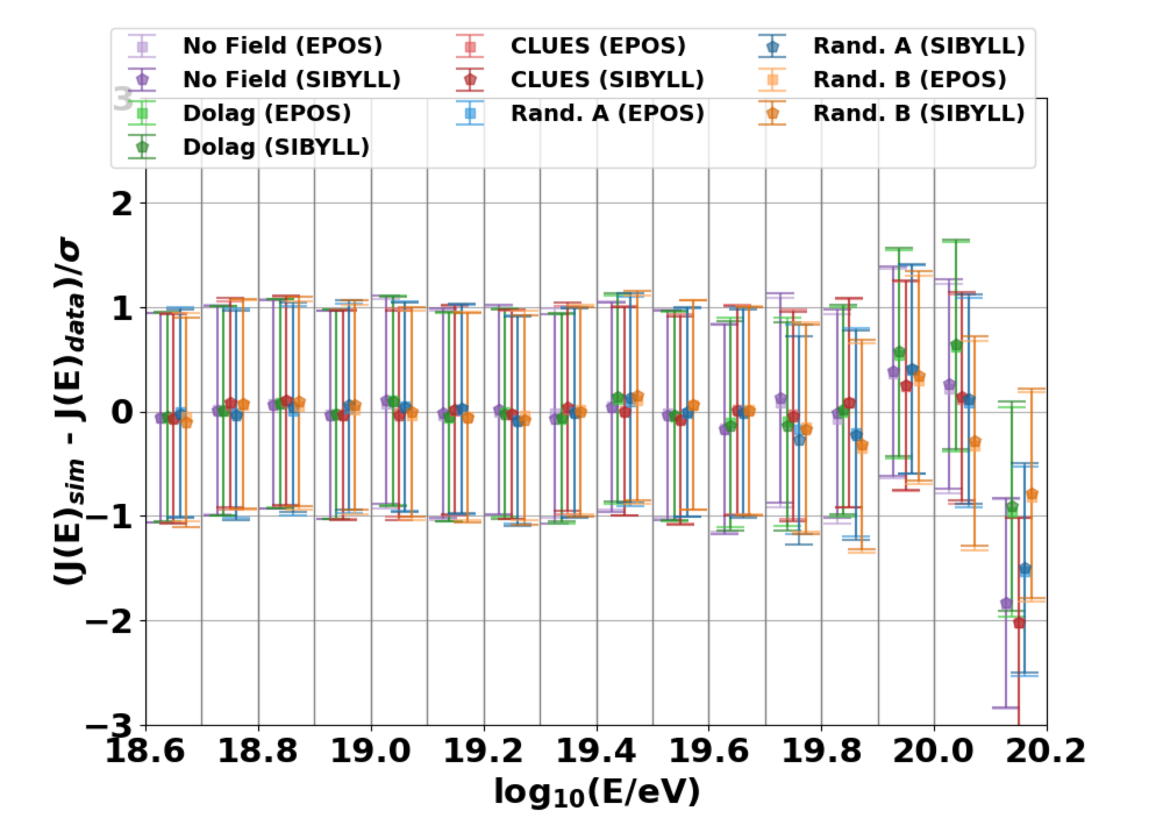

Energy Spectra Residuals for all models

EFFECT OF EXTENDING TO Z = 0.5

- 1 nG 234 kpc MAGNETIC FIELD

Extrapolating **to FR0 sources** ***z = 0.05 to 0.5:***

- **Proton ratio (detected)/(emitted nuclei) is ~1/24th that of z = 0 to 0.05.**
  - **Neutrinos (detected)/(emitted nuclei) is ~1/68th .**
- **Iron ratio is ~1/51th .**
  - **Neutrinos is ~1/26th.**
- **Results: small correction with significant computing penalty** ***so we extended to z = 0.2***

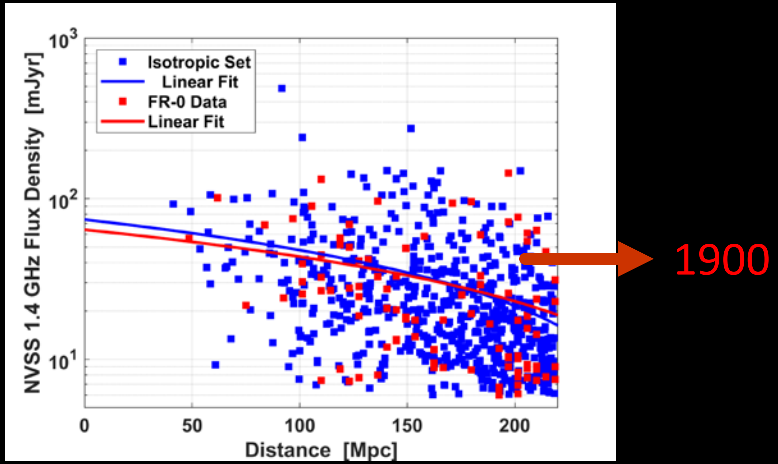

Local source evolution modeled by preserving correlation between radio output and redshift distance (Kendall's correlation coeff.: -0.28, p-Value: 4.6e-5)[1].

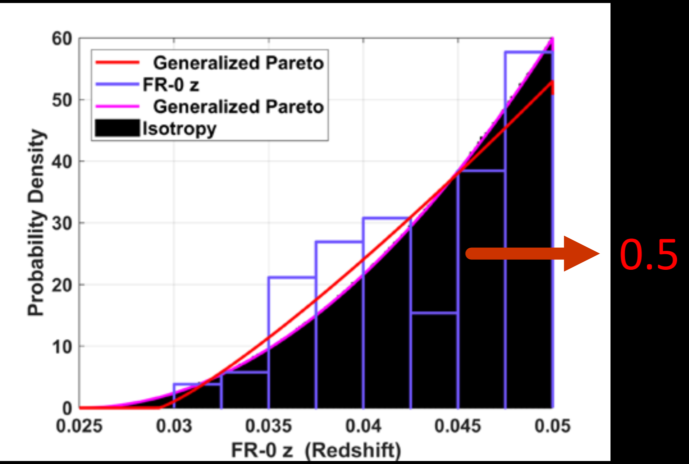

Simulated FR-0 redshift distribution from Pareto fit to catalog data[1]. Isotropy probability of ~16%.

EFFECT OF EXTENDING MAXIMUM Z

- IRON: 1 nG 234 kpc MAGNETIC FIELD

- **Updated CRPropa 3**
- **Extrapolating to FR0 sources z = 0.05 up to 0.5 (simulate 0 to 0.5)**

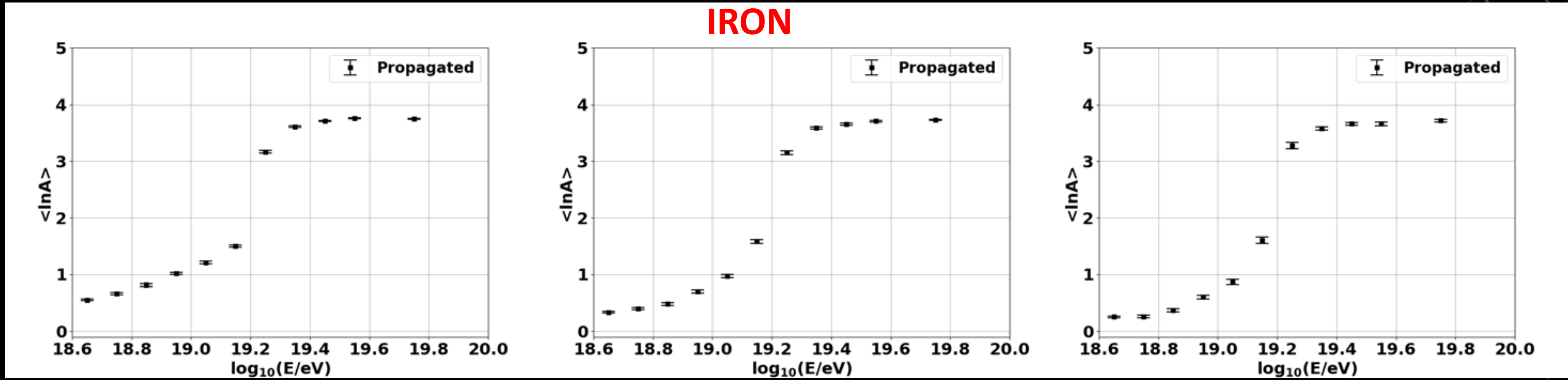

Up to z = 0.05

Up to z = 0.1

Up to z = 0.2

- **Iron propagation does not change significantly past z = 0.1**
- **Up to z = 0.5 has too high computation cost.**

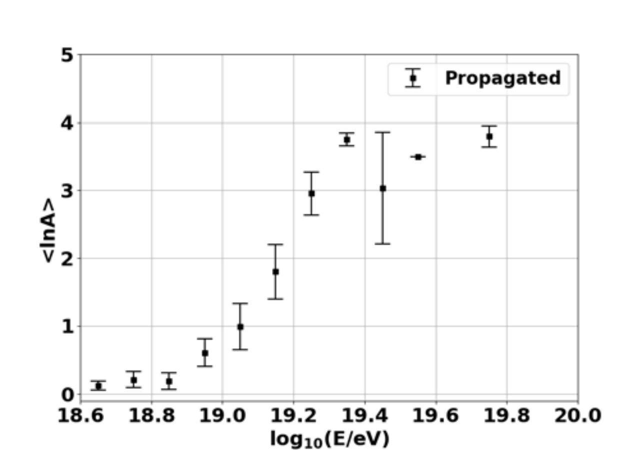

Up to z = 0.5 (smaller stats)

EFFECT OF EXTENDING MAXIMUM Z

– IRON: 1 nG 234 kpc MAGNETIC FIELD

- **Updated CRPropa 3**
- **Extrapolating to FR0 sources z = 0.05 up to 0.5 (simulate 0 to 0.5)**

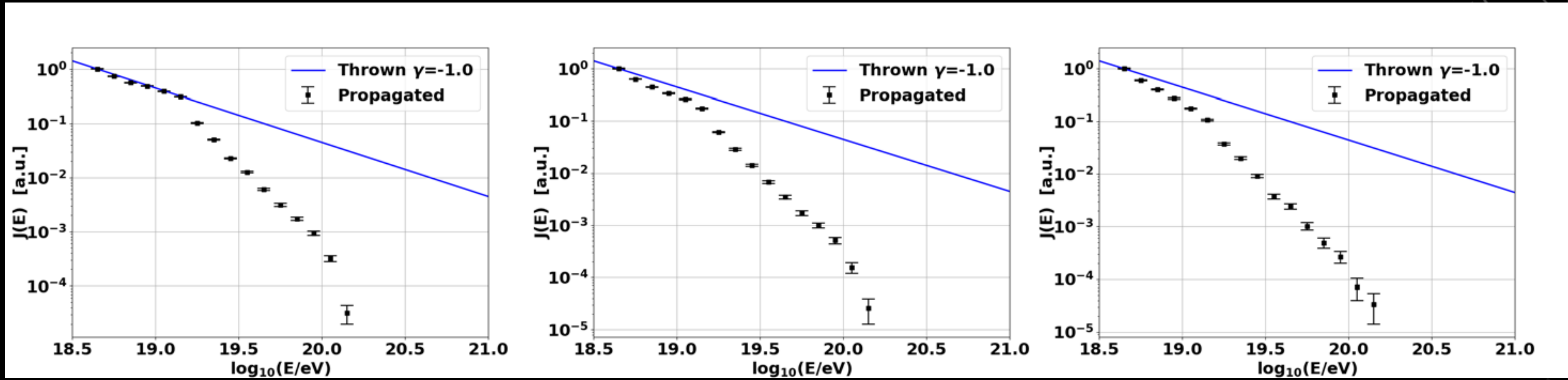

Up to z = 0.05

Up to z = 0.1

Up to z = 0.2

Different scales

- **Iron propagation does not change significantly past z = 0.1**
- **Up to z = 0.5 has too high computation cost.**

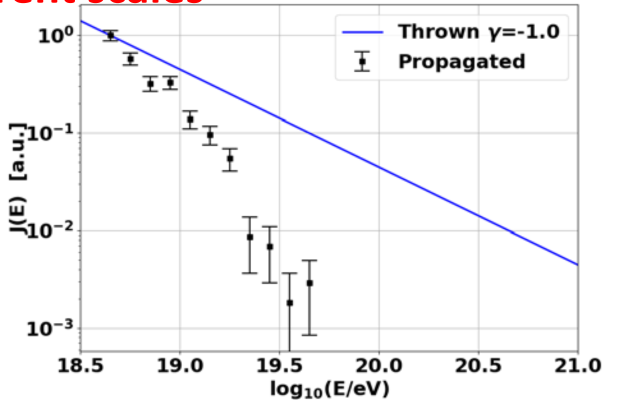

Up to z = 0.5 (smaller stats)

EFFECT OF EXTENDING MAXIMUM Z

– IRON EMITTED NEUTRINOS: 1 nG 234 kpc MAGNETIC FIELD

- **Updated CRPropa 3**
- **Extrapolating to FR0 sources z = 0.05 up to 0.5 (simulate 0 to 0.5)**

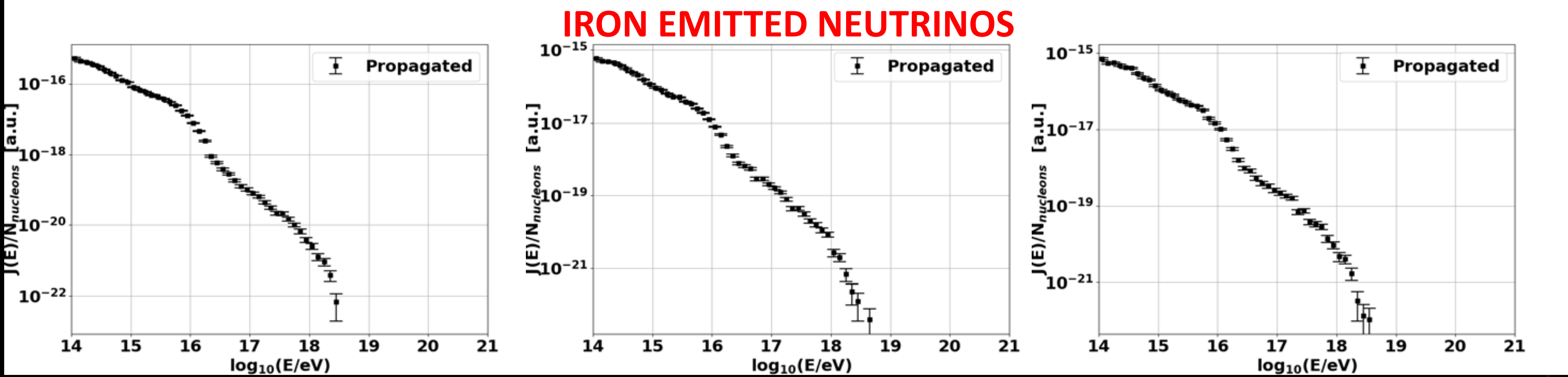

Up to z = 0.05 **Up to z = 0.1** **Up to z = 0.2**

Different scales

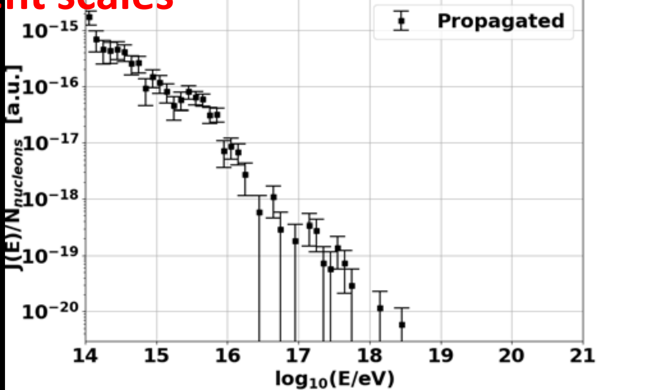

Up to z = 0.5 (smaller stats)

- **Iron propagation does not change significantly past z = 0.1**
- **Up to z = 0.5 has too high computation cost.**

EFFECT OF EXTENDING MAXIMUM Z

- IRON EMITTED NEUTRINOS: 1 nG 234 kpc MAGNETIC FIELD

- **Updated CRPropa 3**
- **Extrapolating to FR0 sources z = 0.05 up to 0.5 (simulate 0 to 0.5)**

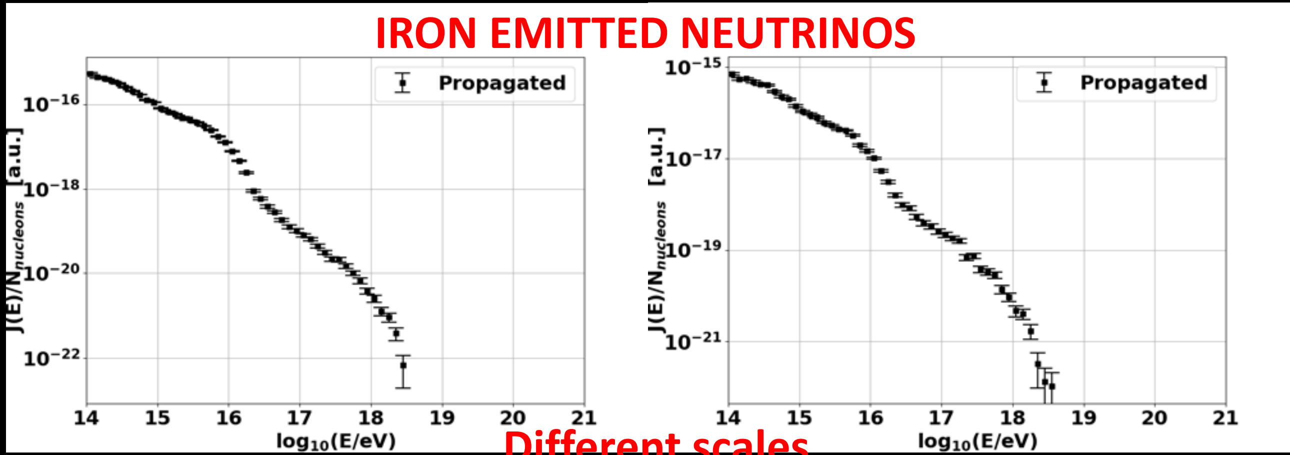

Up to z = 0.05 **Up to z = 0.2**

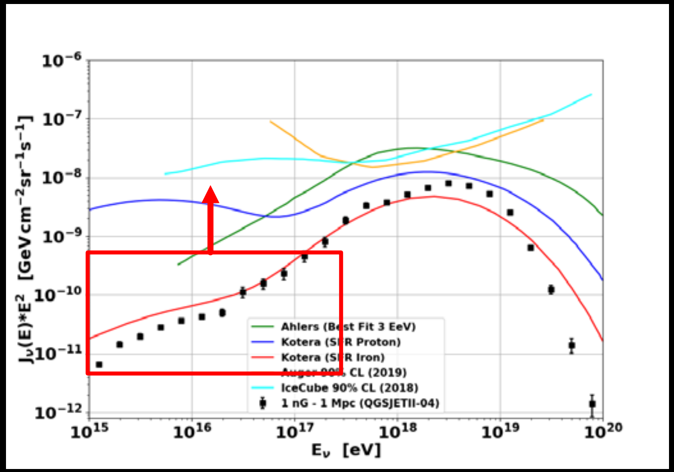

- **More neutrinos.**
  - **Seems to affect lower energy more.**

EVOLVING FRACTION ADDITIONAL

VARIANCE RESULTS

- Var(lnA) for log10(E) from 18.6 to 19.0
  - No field-Sibyll: 2.31 ± 0.07
  - No field-EPOS: 1.97 ± 0.10
  - Dolag-Sibyll: 1.32 ± 0.04
  - Dolag-EPOS: 1.64 ± 0.04
  - CLUES-Sibyll: 1.44 ± 0.06
  - CLUES-EPOS: 1.49 ± 0.05
  - 1ng1mpc-Sibyll: 1.44 ± 0.04
  - 1ng1mpc-EPOS: 1.25 ± 0.07
  - 1ng3mpc-Sibyll: 1.11 ± 0.02
  - 1ng3mpc-EPOS: 0.89 ± 0.03

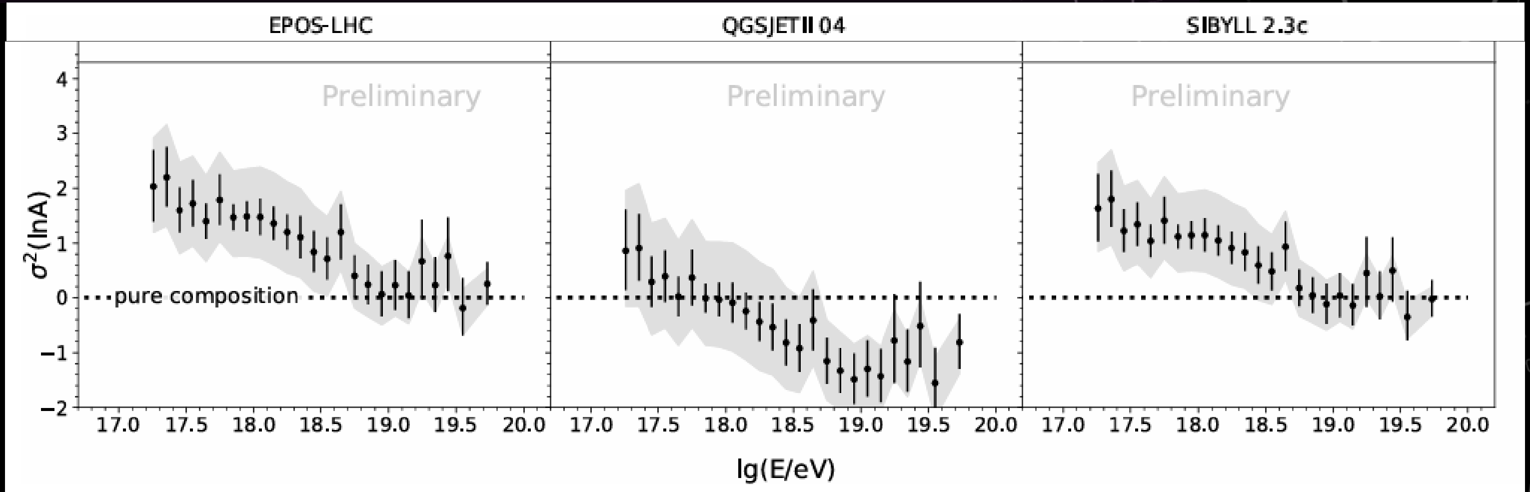

Data for log10(E) from 18.5 to 19.0:
1.64 ± 0.92
Does not include muon uncertainty
Yushkov, A. 2020, PoS, ICRC2019, 482

EVOLVING NUCLEI FRACTIONS (OBSERVED)

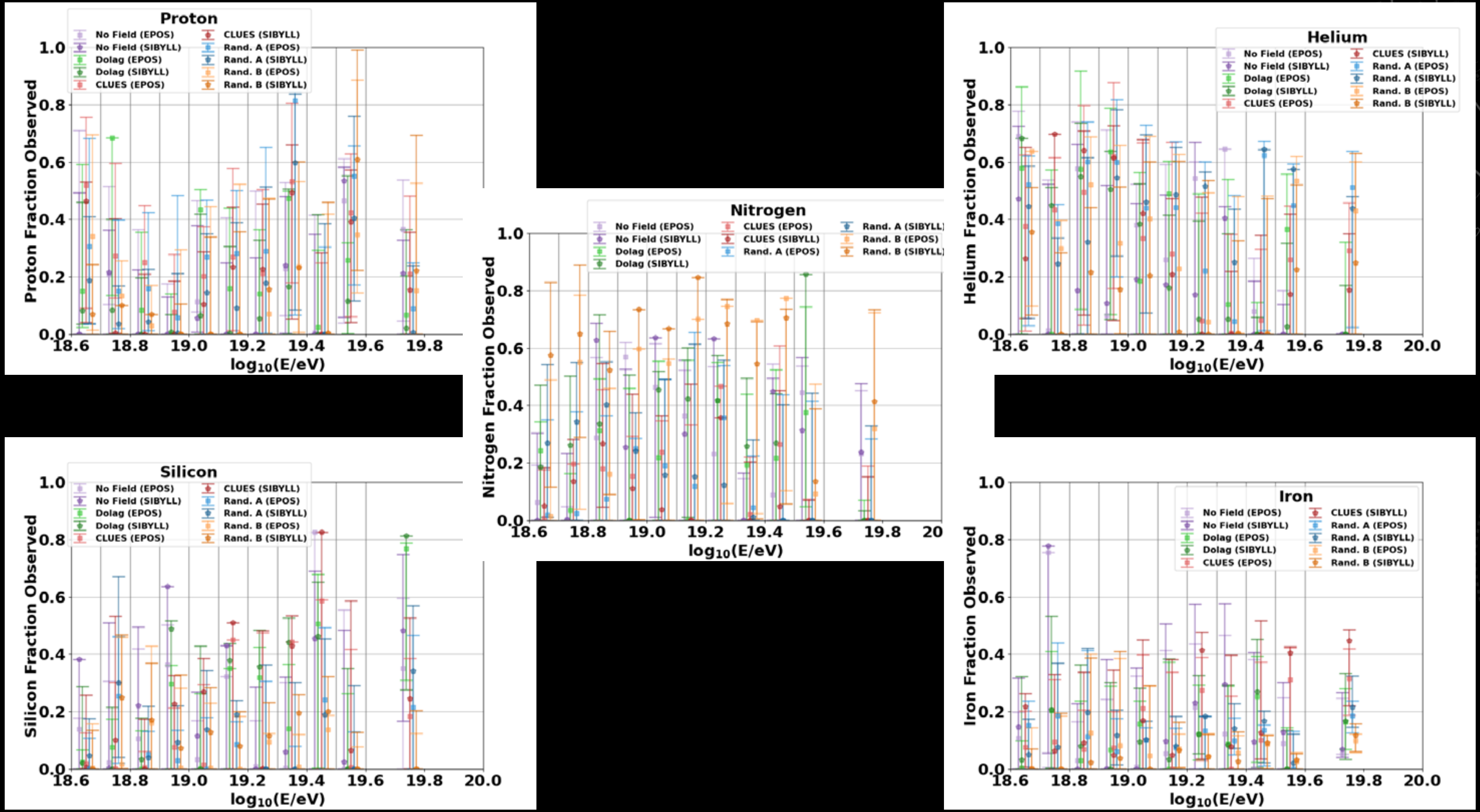

Observed Nuclei Fraction Versus Magnetic Field

SECONDARY RATIOS

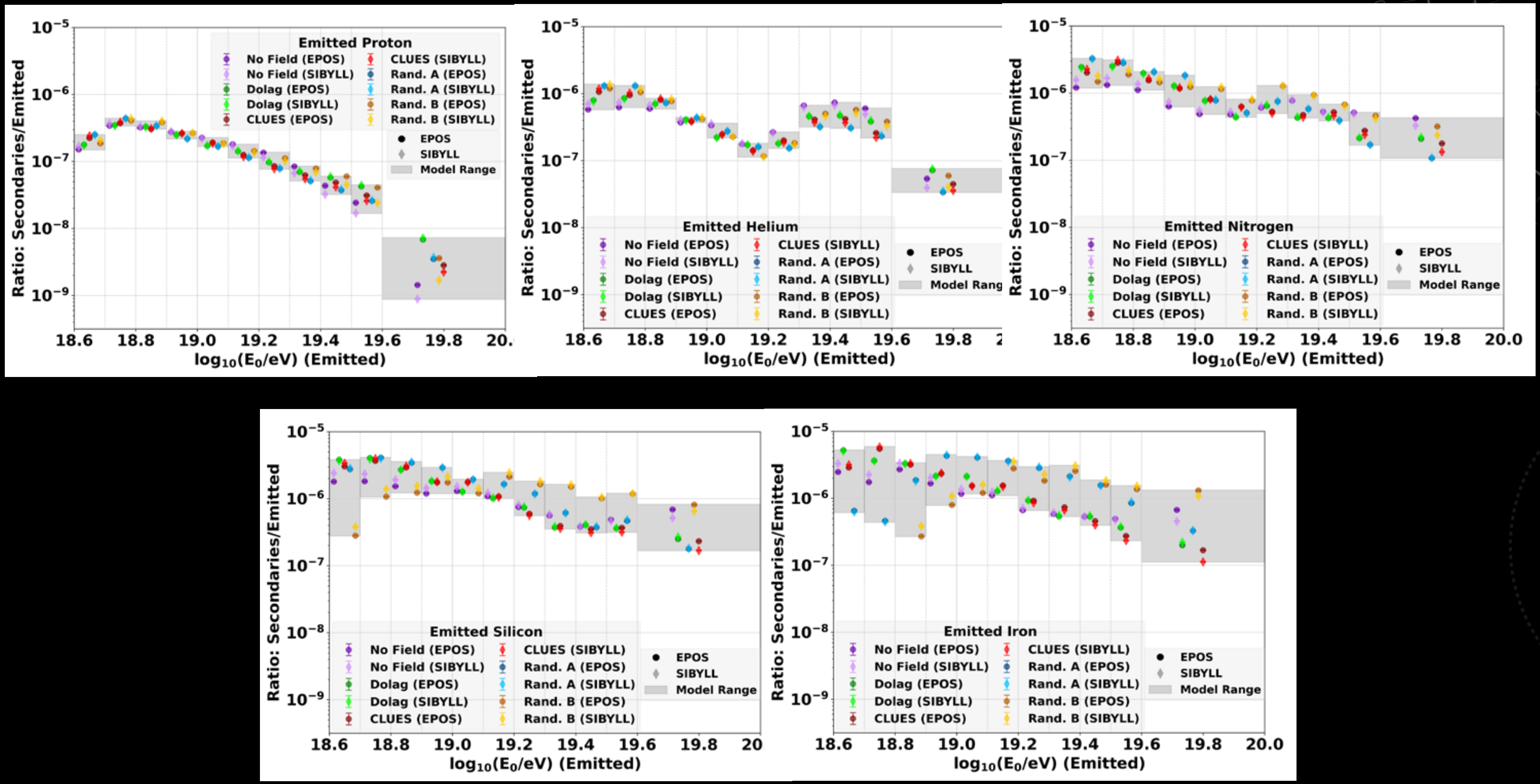

Used to convert observed fractions to emitted fractions

OBSERVED <lnA>

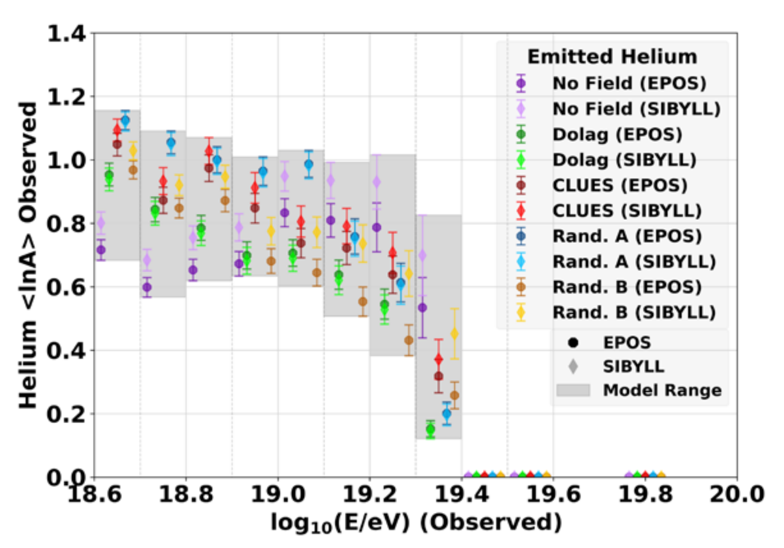

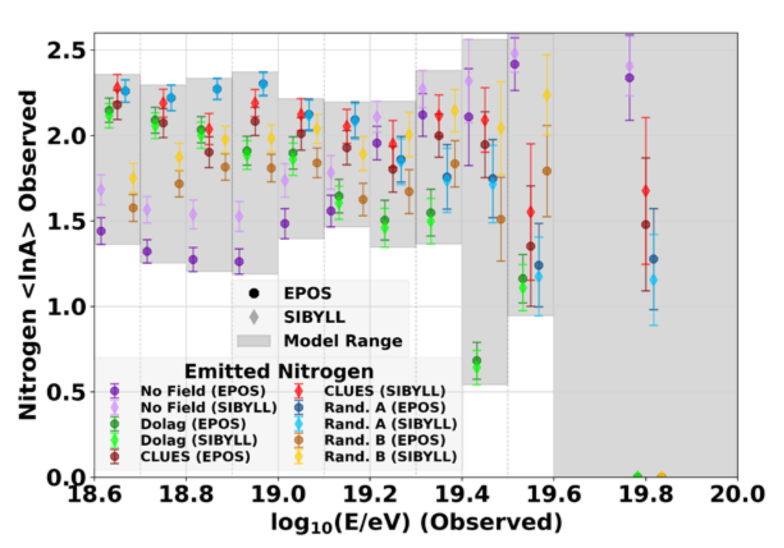

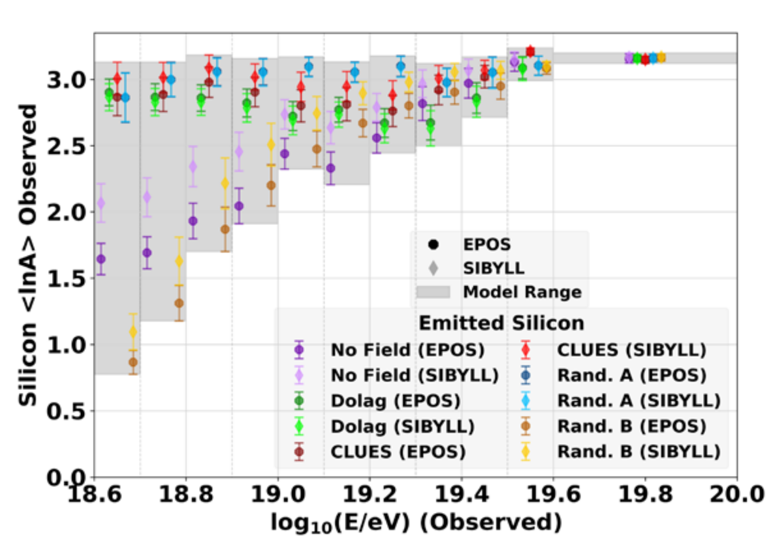

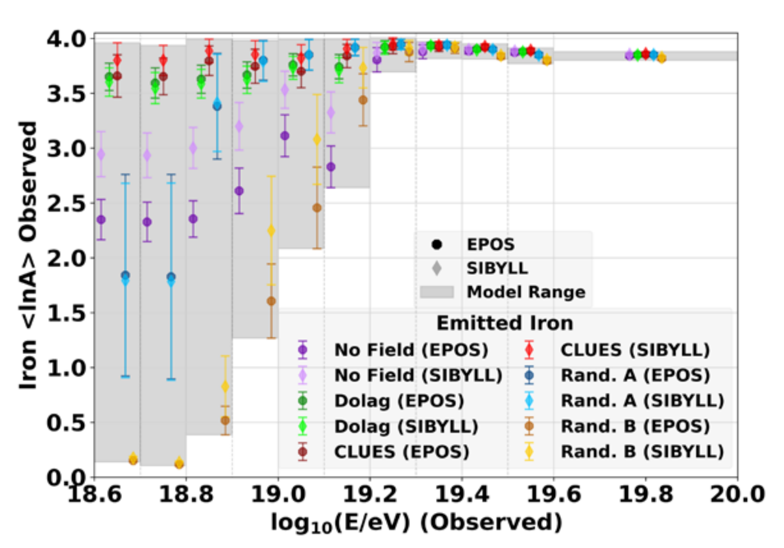

FIT RESULT TABLES

Table 5. Evolving Fraction Energy Spectrum Parameters

Field	Model	$\Sigma\chi^2$/bin	γ	$\log_{10}(R_{cut}/V)$	D_{cut}/Mpc	n
No Field	SIBYLL	0.370	$2.10^{+0.47}_{-0.14}$	$19.19^{+0.84}_{-0.20}$	844^{+0}_{-1}	$1.344^{+0.014}_{-0.005}$
	EPOS	0.326	$1.94^{+0.60}_{-0}$	$19.22^{+0.75}_{-0.01}$	844^{+0}_{-1}	$1.343^{+0.006}_{-0.005}$
Dolag	SIBYLL	0.469	$2.28^{+0.14}_{-0.84}$	$19.89^{+0.31}_{-0.98}$	907^{+450}_{-50}	$1.328^{+0.023}_{-0.000}$
	EPOS	0.446	$2.31^{+0.12}_{-0.20}$	$19.89^{+0.40}_{-0.38}$	889^{+146}_{-39}	$1.342^{+0.006}_{-0.011}$
CLUES	SIBYLL	0.307	$2.65^{+0.00}_{-0.29}$	$19.58^{+0.27}_{-0.25}$	841^{+1}_{-0}	$1.342^{+0.013}_{-0.007}$
	EPOS	0.295	$2.52^{+0.09}_{-0.22}$	$19.58^{+0.51}_{-0.20}$	842^{+0}_{-1}	$1.342^{+0.006}_{-0.004}$
Rand.A	SIBYLL	0.344	$2.64^{+0.20}_{-0.25}$	$19.95^{+0.50}_{-0.56}$	855^{+93}_{-7}	$1.343^{+0.008}_{-0.005}$
	EPOS	0.341	$2.65^{+0.05}_{-0.30}$	$19.89^{+0.94}_{-0.32}$	844^{+113}_{-0}	$1.342^{+0.006}_{-0.006}$
Rand.B	SIBYLL	0.236	$2.35^{+0.34}_{-0.30}$	$19.40^{+1.64}_{-0.32}$	843^{+171}_{-0}	$1.346^{+0.009}_{-0.006}$
	EPOS	0.237	$2.21^{+0.34}_{-0.45}$	$19.51^{+1.20}_{-0.38}$	843^{+174}_{-0}	$1.342^{+0.004}_{-0.007}$

Notes. The FR0 evolving fraction combined fit results total sum chi-square per bin, spectral index γ, exponential rigidity cutoff ($\log_{10}(R_{cut}/V)$), trajectory cutoff (D_{cut}), and spectrum normalization for all 10 configurations. The two EAS are EPOS-LHC (EPOS) and Sibyll2.3c (SIBYLL).

FIT RESULT TABLES

Table 6. Evolving Fraction Bootstrap Energy Spectrum Parameters

Field	Model	$\Sigma\chi^2$/bin	γ	$\log_{10}(R_{cut}/V)$	D_{cut}/Mpc	n
No Field	SIBYLL	0.370	$2.44^{+0.23}_{-0.23}$	$19.34^{+0.25}_{-0.25}$	843^{+0}_{-0}	$1.345^{+0.006}_{-0.006}$
	EPOS	0.326	$2.47^{+0.12}_{-0.12}$	$19.40^{+0.10}_{-0.10}$	843^{+0}_{0}	$1.340^{+0.004}_{-0.004}$
Dolag	SIBYLL	0.469	$2.26^{+0.28}_{-0.28}$	$19.23^{+0.25}_{-0.25}$	867^{+193}_{-193}	$1.335^{+0.004}_{-0.004}$
	EPOS	0.446	$2.26^{+0.19}_{-0.19}$	$19.74^{+0.18}_{-0.18}$	890^{+107}_{-107}	$1.341^{+0.003}_{-0.003}$
CLUES	SIBYLL	0.307	$2.40^{+0.07}_{-0.07}$	$19.71^{+0.12}_{-0.12}$	842^{+0}_{-0}	$1.347^{+0.013}_{-0.007}$
	EPOS	0.295	$2.34^{+0.06}_{-0.06}$	$19.68^{+0.10}_{-0.10}$	842^{+0}_{-0}	$1.341^{+0.005}_{-0.005}$
Rand.A	SIBYLL	0.344	$2.37^{+0.05}_{-0.05}$	$19.83^{+0.11}_{-0.11}$	853^{+35}_{-35}	$1.342^{+0.003}_{-0.003}$
	EPOS	0.341	$2.33^{+0.05}_{-0.05}$	$19.68^{+0.08}_{-0.08}$	851^{+30}_{-30}	$1.342^{+0.003}_{-0.003}$
Rand.B	SIBYLL	0.236	$2.41^{+0.10}_{-0.10}$	$19.74^{+0.41}_{-0.41}$	850^{+43}_{-43}	$1.348^{+0.004}_{-0.004}$
	EPOS	0.237	$2.31^{+0.11}_{-0.11}$	$19.59^{+0.20}_{-0.20}$	853^{+49}_{-49}	$1.345^{+0.004}_{-0.004}$

Notes. The FR0 evolving fraction combined fit bootstrap distribution most probable spectral index γ, exponential rigidity cutoff ($\log_{10}(R_{cut}/V)$), trajectory cutoff (D_{cut}), and spectrum normalization for all 10 configurations.